Inert and growing thin shells

Mode of deformation of two vegetal thin shells: a seedpod and a pollen grain.

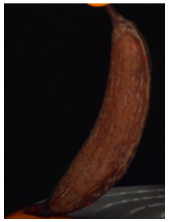

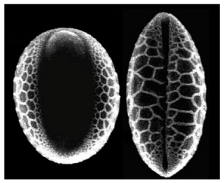

E Couturier[1,5]

E Couturier[1], E Cerda[1], J Dumais[2], E Katifori[3]

Growth and division of a fungal thin shell: the fission yeast.

JF Abenza-Martinez[4], E Couturier[1,5], J Dumais[3], RE Carazo-Salas

1: USACH Santiago
3: UAI Viña del Mar
3: MPI Göttingen
4: : Gurdon Institute Cambridge
5: MSC Paris Diderot

A polen grain and a seedpod

Open

Pollen grain

Dianella caerula

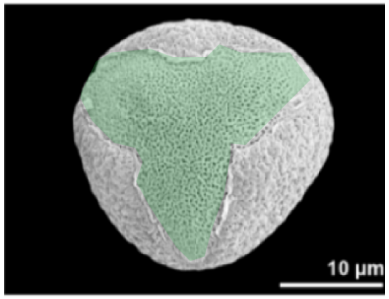

Seedpod.

Acaccia caven

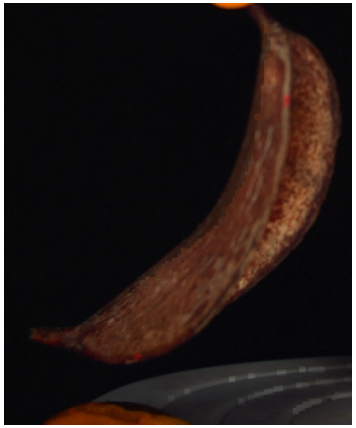

Changing the humidity triggers the sealing of the thin shell

Open

Self-sealed

Pollen grain

Dianella caerula

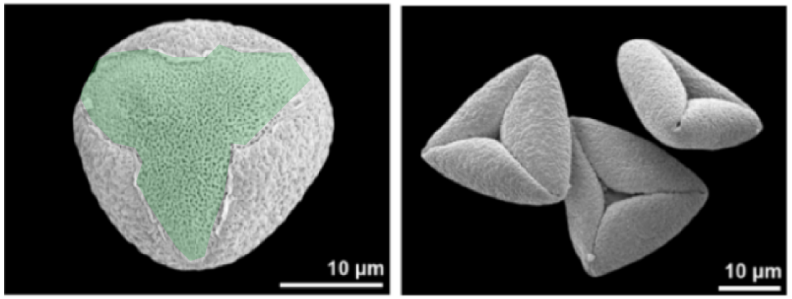

Seedpod.

Acaccia caven

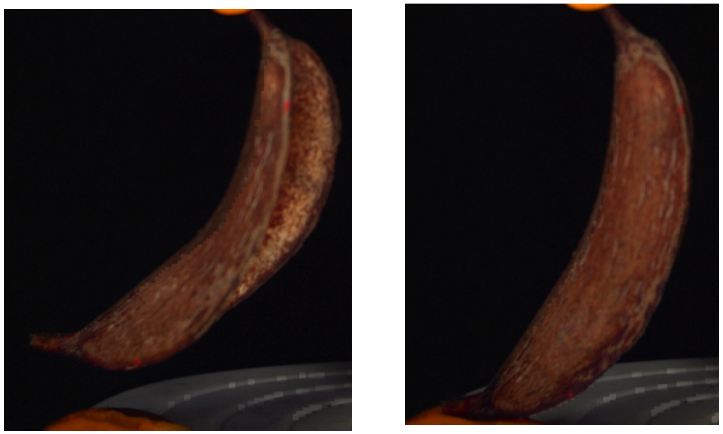

Isometric deformations ?

Isometric mode are the most favorable for the energy when possible

(Jellett 1849)

Open

Self-sealed

Pollen grain

Dianella caerula

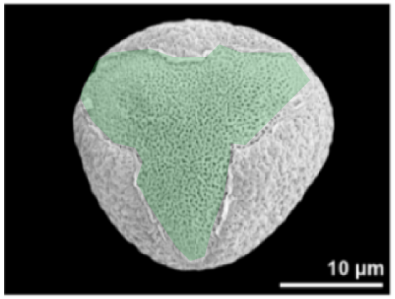

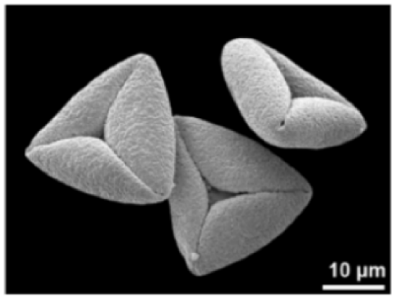

Seedpod.

Acaccia caven

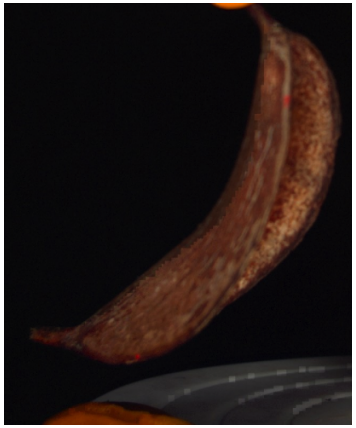

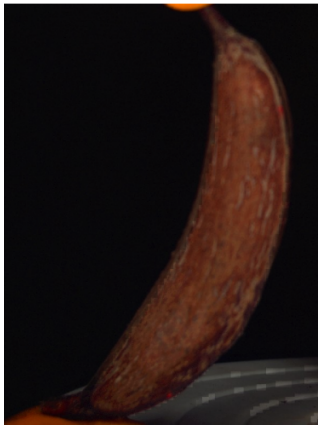

Isometric deformations ?

Isometric mode are the most favorable for the energy when possible

(Jellett 1849)

Open | Self-sealed

Pollen grain

Dianella caerula

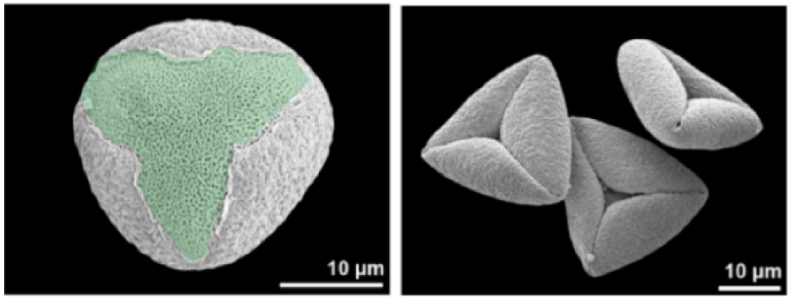

Convex shell with a hole.
Isometry possible on some range.

Seedpod.

Acaccia caven

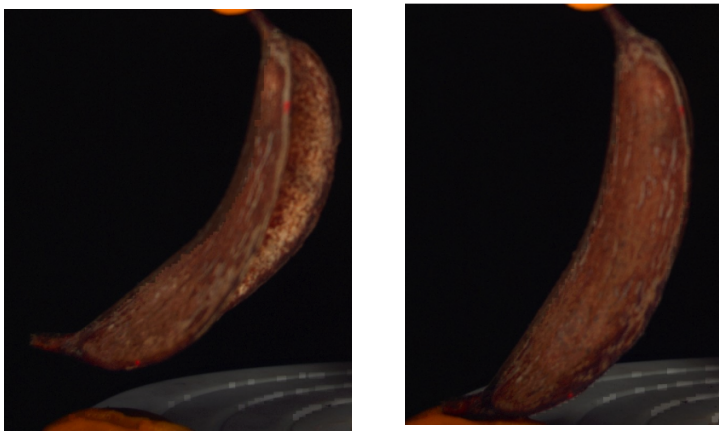

Isometric deformations ?

Isometric mode are the most favorable for the energy when possible

(Jellett 1849)

Open Self-sealed

Pollen grain

Dianella caerula

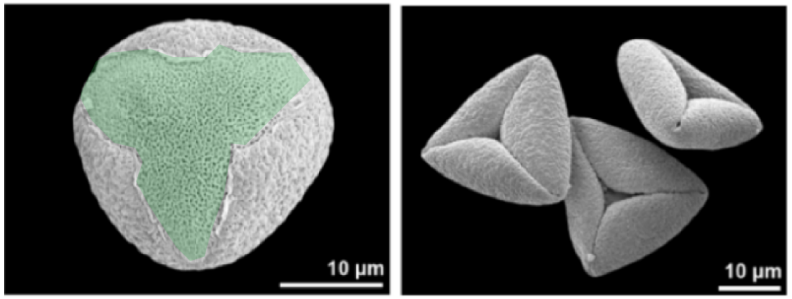

Convex shell with a hole.
Isometry possible on some range.

Seedpod.

Acaccia caven

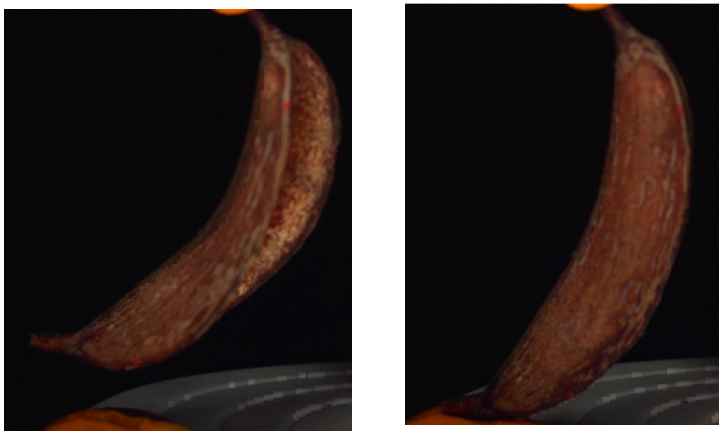

Non convex shell.
Isometry not always possible.

(Spivak for instance).

Isometric deformations ?

Isometric mode are the most favorable for the energy when possible (Jellett 1849)

Open | Self-sealed

Pollen grain

Dianella caerula

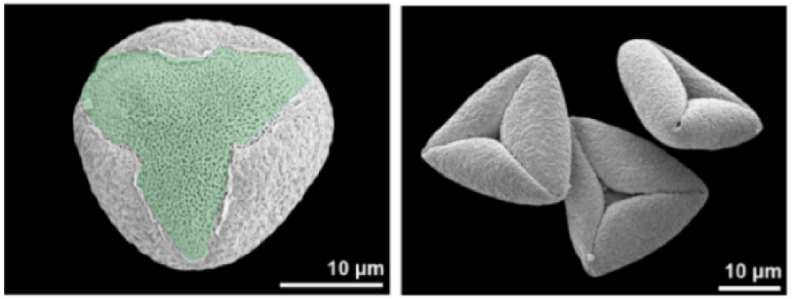

Convex shell with a hole.
Isometry possible on some range.

Seedpod.

Acaccia caven

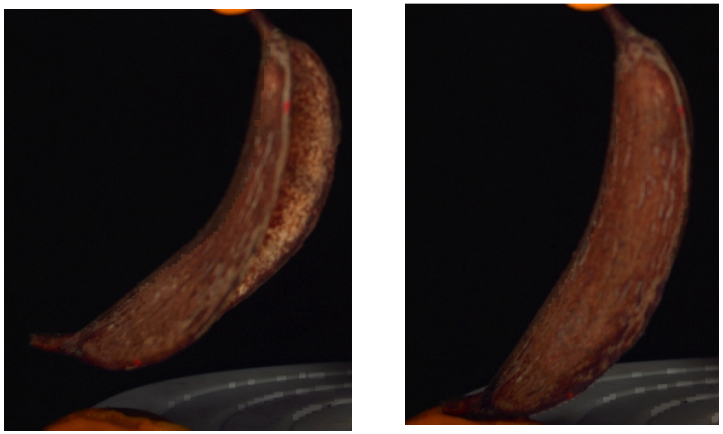

Non convex shell.
Isometry not always possible.

(Spivak for instance).

Review the existing work (1890-1930) and adapt it to understand the rules behind the design of these self-sealing thin shells

Folded Goursat surfaces and banana-shaped seedpod.

Gaussian curvature

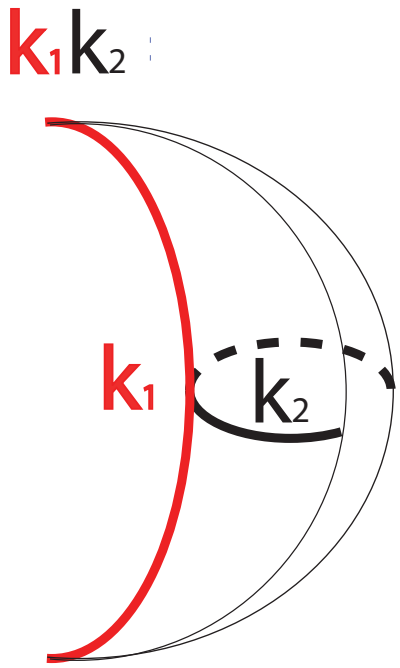

Gaussian curvature is conserved by isometric deformations

$k_1 k_2 = \text{Cste}$

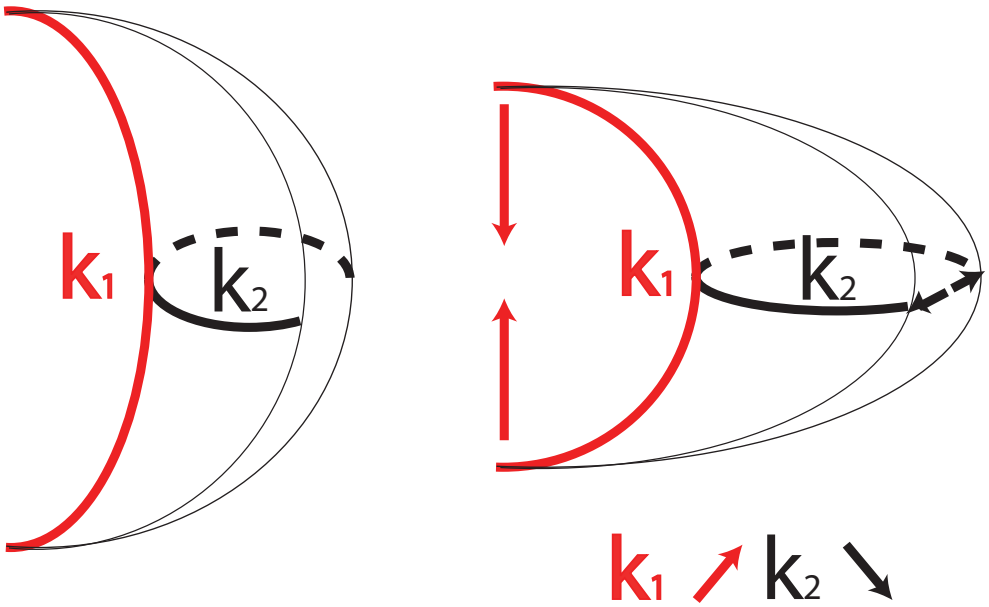

Gaussian curvature is conserved by isometric deformations

$k_1 k_2 = \text{Cste}$

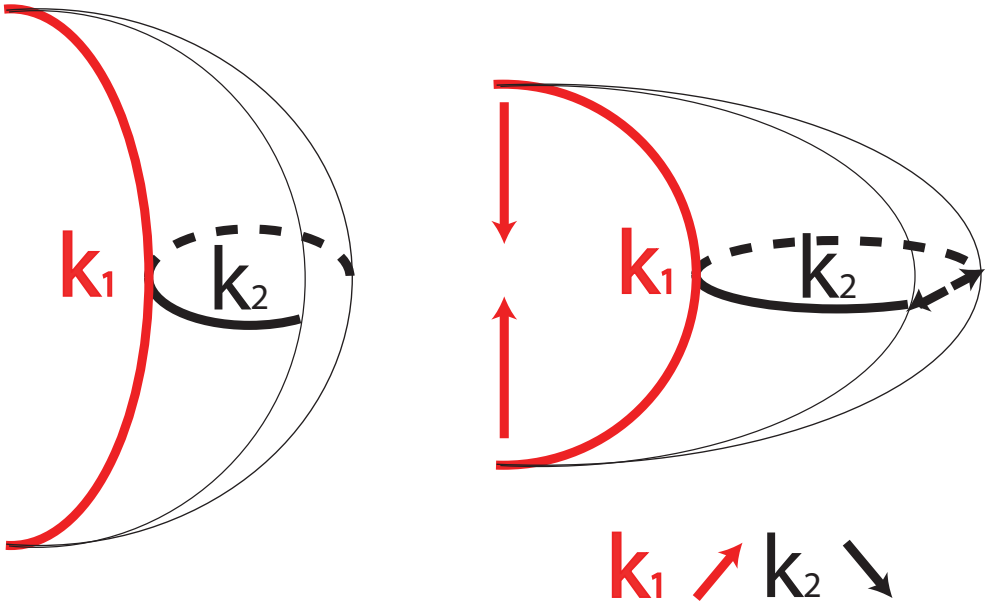

Idea of J Dumais and E Cerda

An elegant LOCAL scenario at the saddle point for the opening.
Does it correspond to a GLOBAL solution ?

A banana shaped family of surface

$$x_0 = c(a + \cos(u))\cos(v)$$

$$y_0 = c\sin(u)\cos(v)$$

$$z_0 = d\sin(v)$$

Upper view

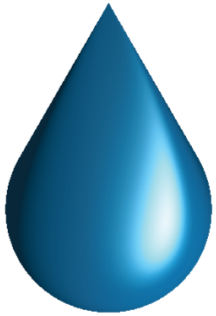

Oblique view

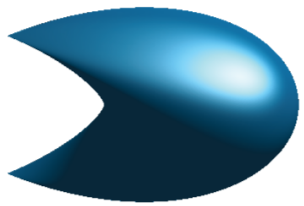

Side view

A mirror symetry

S*=
Half of S +
mirror symetric of the other
half of S

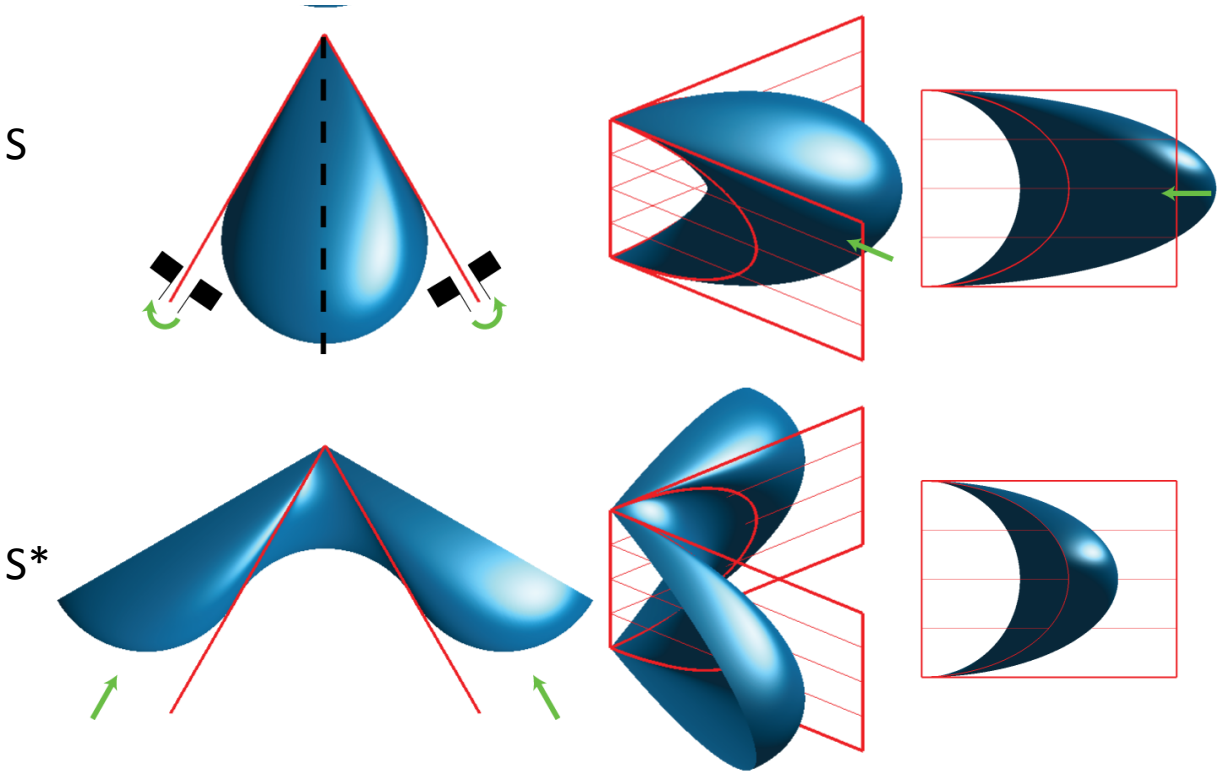

As the mirror plane is tangent to the surface, there is neither a fold in S nor in S*.

A mirror symetry

S*=
Half of S +
mirror symetric of the other
half of S

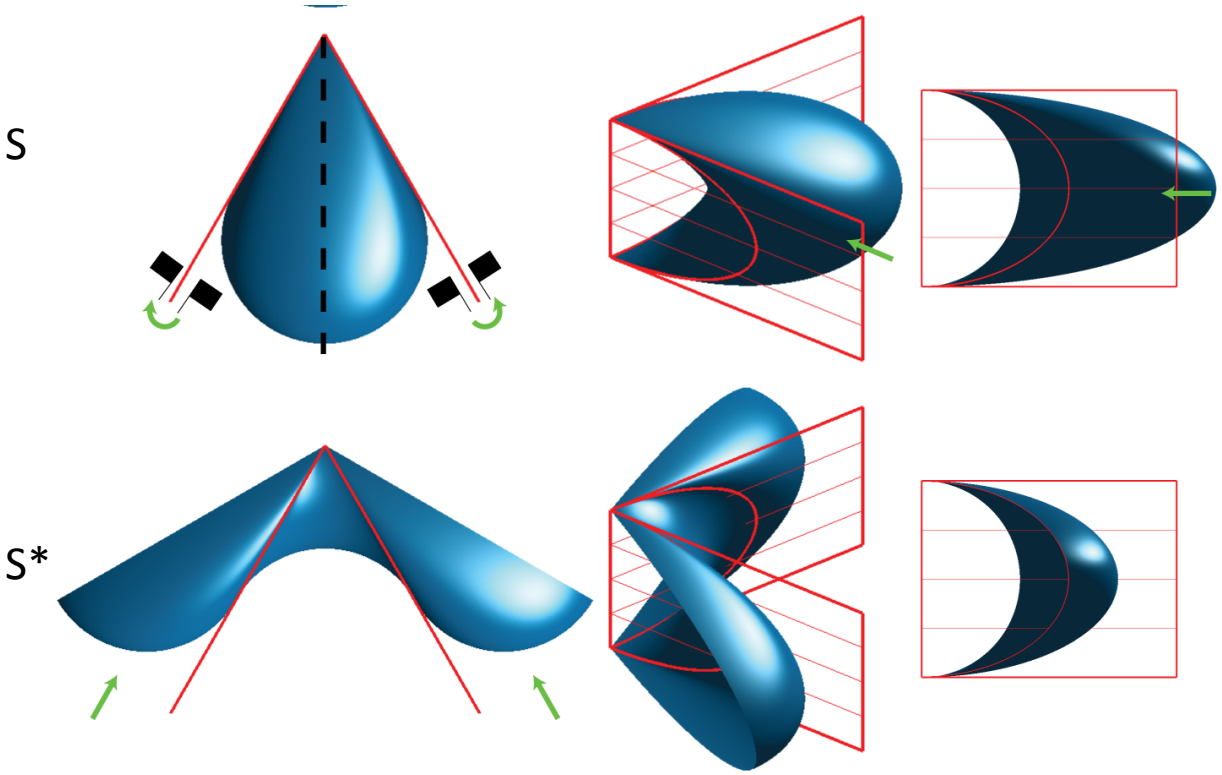

S* admits a one-parameter C∞ family of isometric deformation S^*_h (Goursat 1891)

$$x_h^* = c\sqrt{1+a^2+2a\cos(u)+h}\cos(v)\cos(\theta_h^*)$$

$$y_h^* = c\sqrt{1+a^2+2a\cos(u)+h}\cos(v)\sin(\theta_h^*)$$

$$z_h^* = \int \sqrt{c^2\cos(v)^2 - hd^2\sin(v)^2}dv$$

$$\theta_h^* = \int \frac{\sqrt{(1+a\cos(u))^2+h}}{1+a^2+2a\cos(u)+h}du$$

The intersection of the surface with any of the planes containing the axis remains in a plane during the isometric deformation.

h=0 → h

Upper view

Oblique view

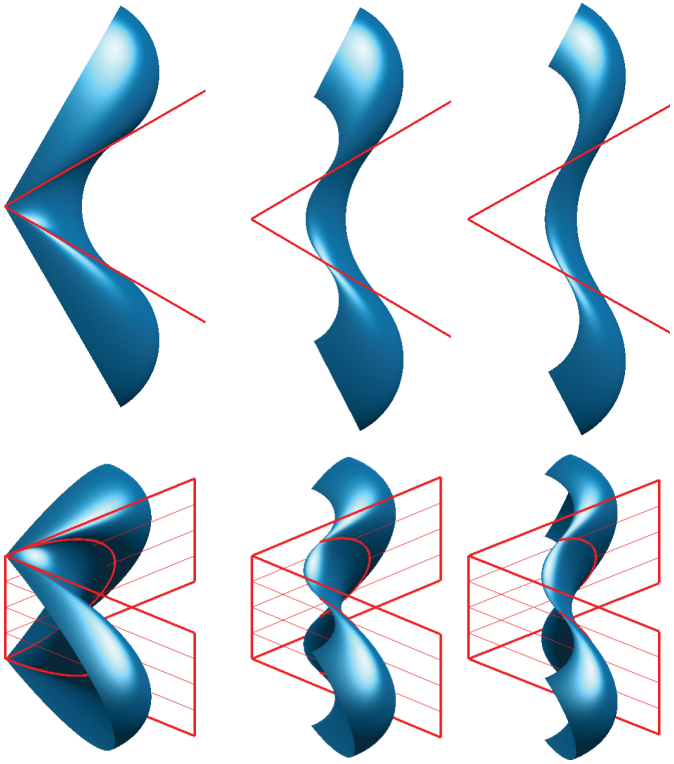

$$x_h^* = c\sqrt{1 + a^2 + 2a\cos(u) + h}\cos(v)\cos(\theta_h^*)$$

$$y_h^* = c\sqrt{1 + a^2 + 2a\cos(u) + h}\cos(v)\sin(\theta_h^*)$$

$$z_h^* = \int \sqrt{c^2\cos(v)^2 - hd^2\sin(v)^2}dv$$

$$\theta_h^* = \int \frac{\sqrt{(1 + a\cos(u))^2 + h}}{1 + a^2 + 2a\cos(u) + h}du$$

The intersection of the surface with any of the planes containing the axis remains in a plane during the isometric deformation.

h=0 → h

Upper view

Oblique view

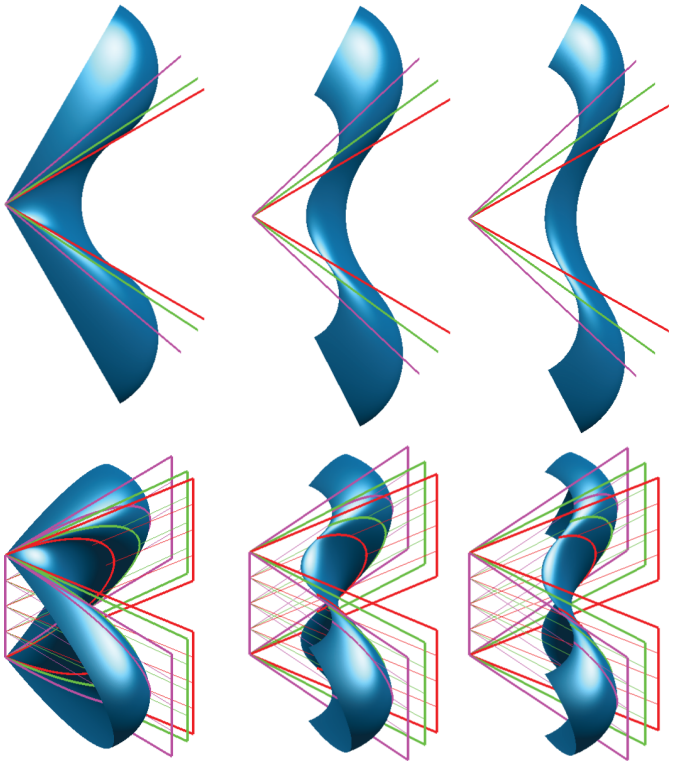

$$x_h^* = c\sqrt{1 + a^2 + 2a\cos(u) + h}\cos(v)\cos(\theta_h^*)$$

$$y_h^* = c\sqrt{1 + a^2 + 2a\cos(u) + h}\cos(v)\sin(\theta_h^*)$$

$$z_h^* = \int \sqrt{c^2\cos(v)^2 - hd^2\sin(v)^2}dv$$

$$\theta_h^* = \int \frac{\sqrt{(1 + a\cos(u))^2 + h}}{1 + a^2 + 2a\cos(u) + h}du$$

To each plane containing the axis corresponds by mirror-symetry a one-parameter family of isometric deformation with a stable curved fold.

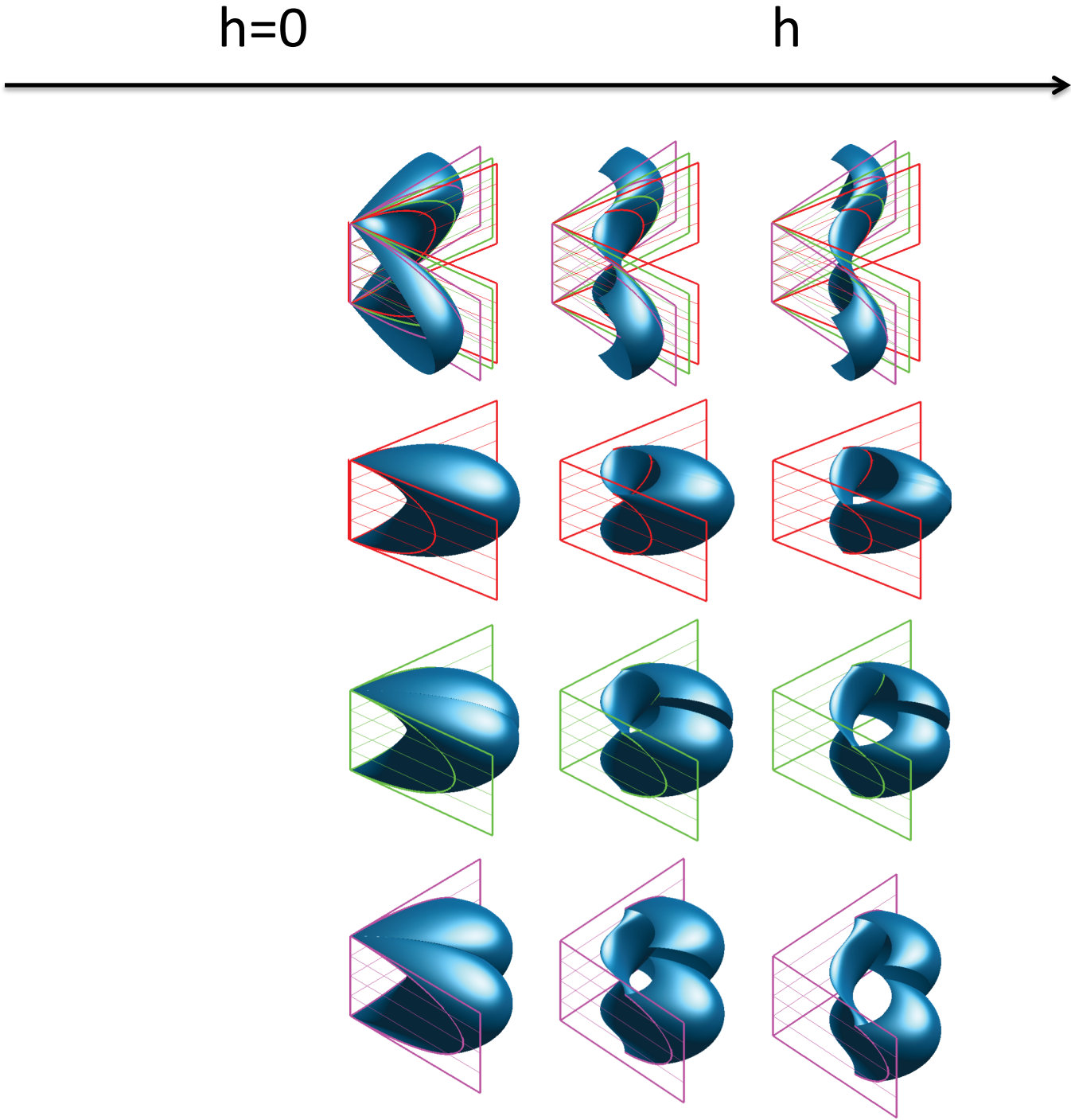

To each plane
containing the axis
corresponds by
mirror-symetry
a one-parameter
family of isometric
deformation with
a stable curved fold.

Gluing the isometric
surfaces on both side of
the fold **imposes**
the opening angle.

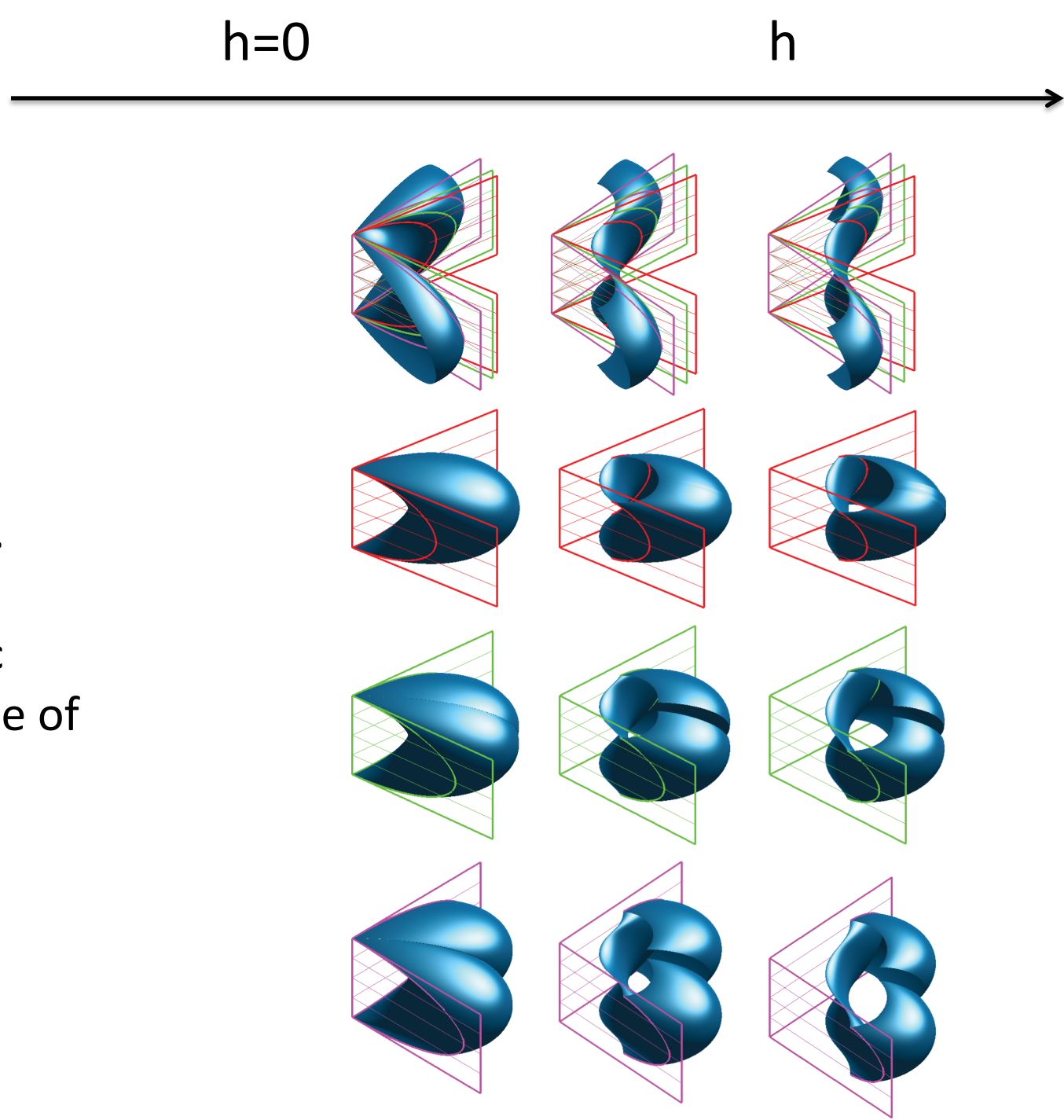

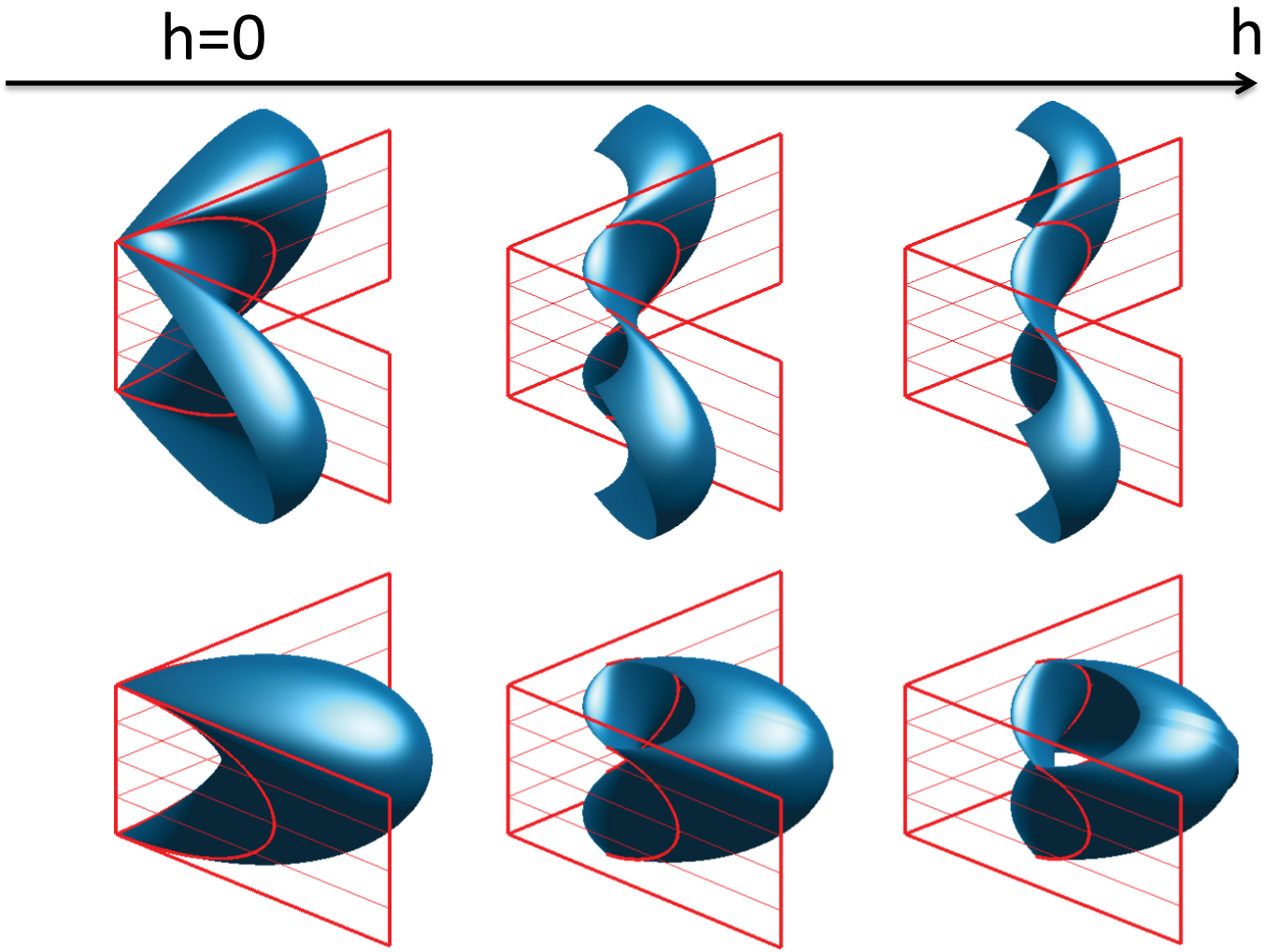

For h=0, the mirror-plane giving the banana solution is **tangently** intersecting the Goursat surface: **No fold.**

For h>0, the mirror-plane giving the banana solution is **transversally** intersecting the Goursat surface: **A fold.**

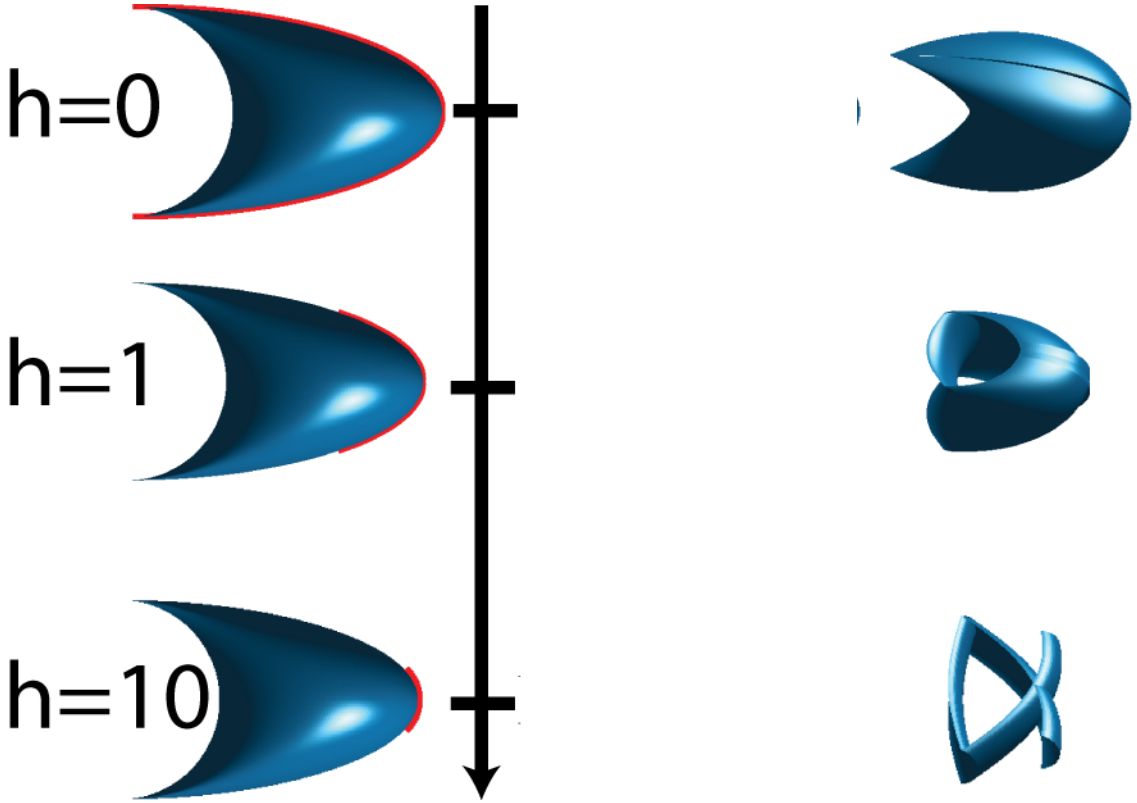

z_h can become imaginary

$h_{max}(v)=c^2/d^2\text{cotan}(v)^2$

$$x_h = c\sqrt{1 + a^2 + 2a\cos(u) + h}\cos(v)\cos(\theta_h)$$

$$y_h = c\sqrt{1 + a^2 + 2a\cos(u) + h}\cos(v)\sin(\theta_h)$$

$$z_h = \int \sqrt{c^2\cos(v)^2 - hd^2\sin(v)^2}dv$$

$$\theta_h = \int sign(1 + a\cos(u))\frac{\sqrt{(1 + a\cos(u))^2 + h}}{1 + a^2 + 2a\cos(u) + h}du$$

Analytical tools for the design

The width of the aperture necessary to close the shell at a prescribed vertical deformation.

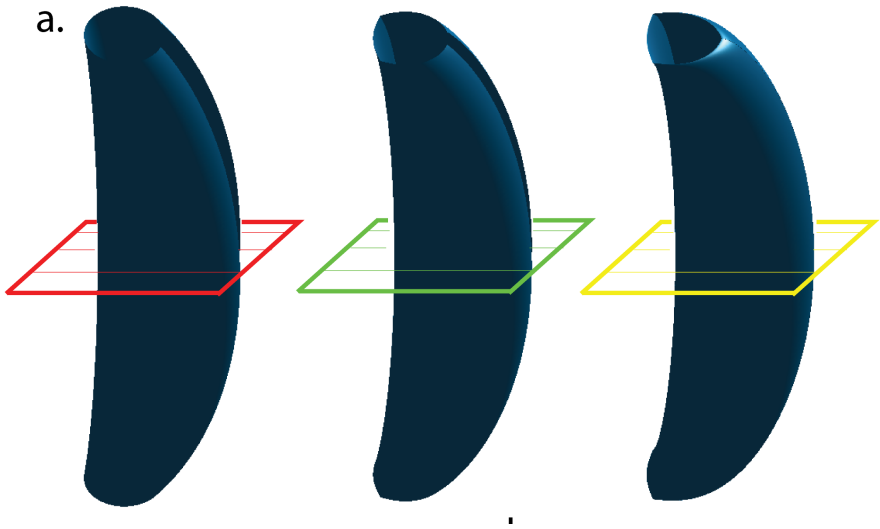

Analytical tools for the design

The width of the aperture necessary to close the shell at a prescribed vertical deformation.

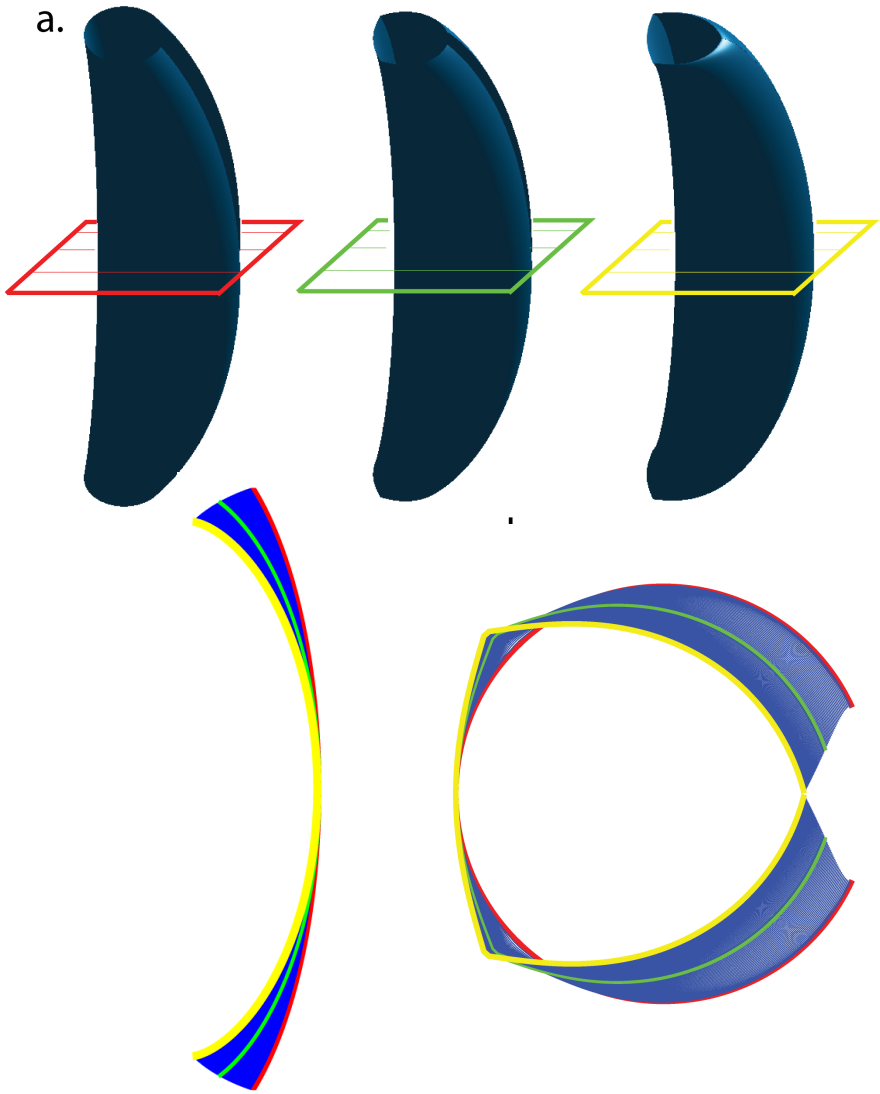

LOCALY (In the saddle point) behave similarly to the the seedpod but not GLOBALY.
Due to the fold the shell closes and does not open.

Longitudinal section at the saddle point

Meridional section

Curvature and energy are analytical

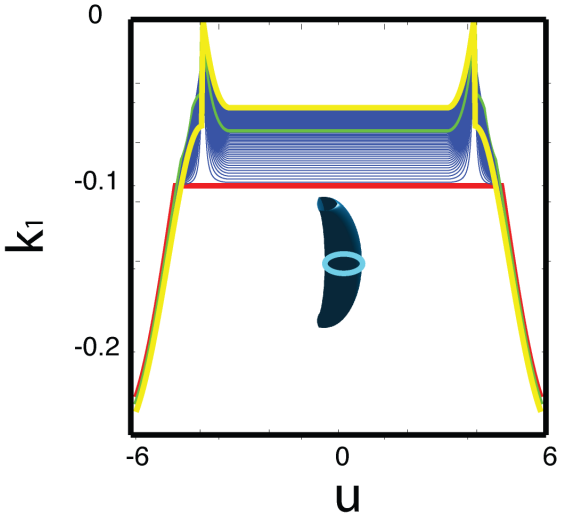

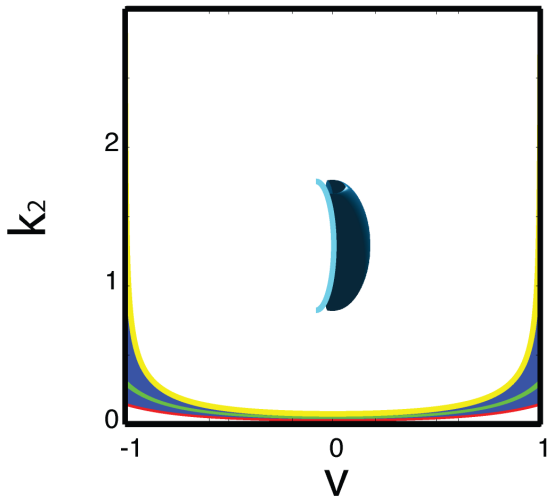

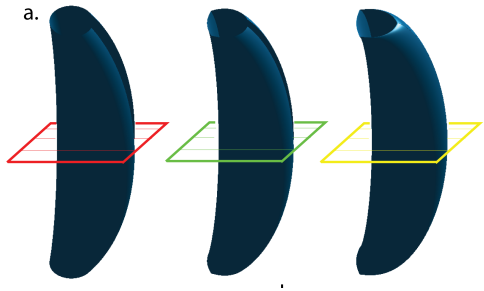

Curvature and energy are analytical

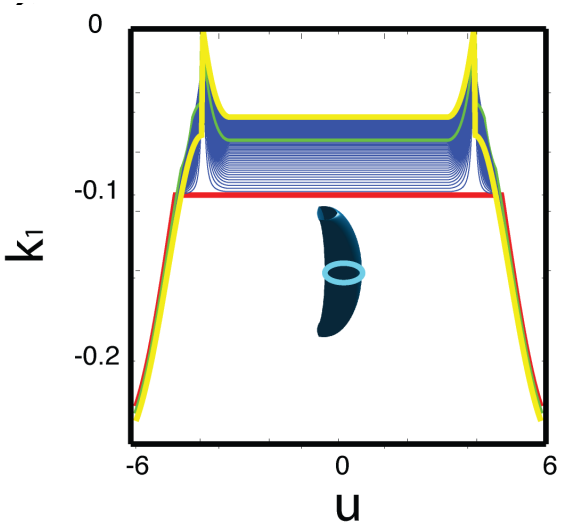

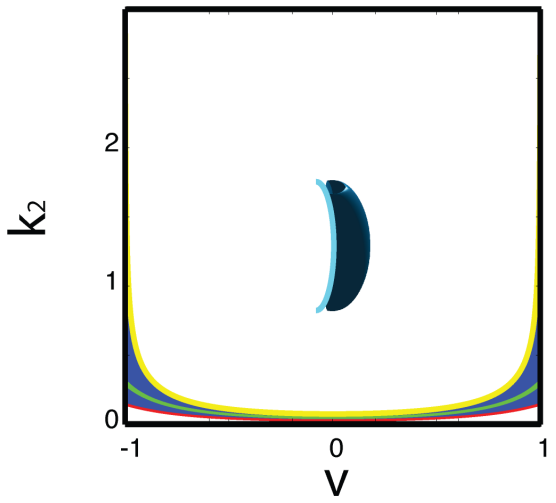

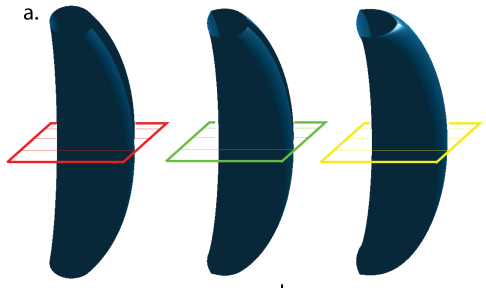

Pure bending energy

$$E_b = \int_u \int_v B\Big((\kappa_1 - \kappa_{10})^2 + 2\nu(\kappa_1 - \kappa_{10})(\kappa_2 - \kappa_{20}) + (\kappa_2 - \kappa_{20})^2\Big)\sqrt{EG - F^2}\,dudv$$

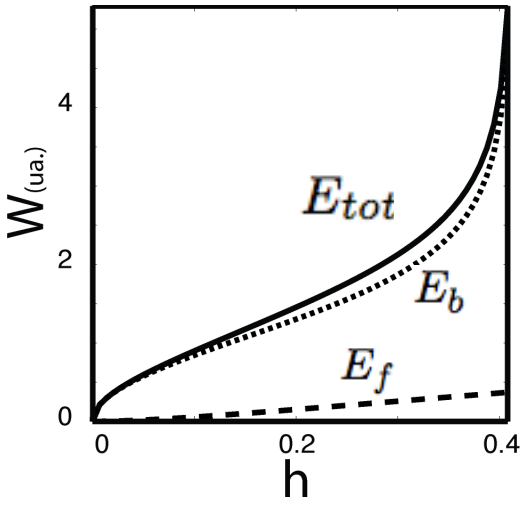

Divergence of k_2 at h_{max} and divergence of E_b

Curvature and energy are analytical

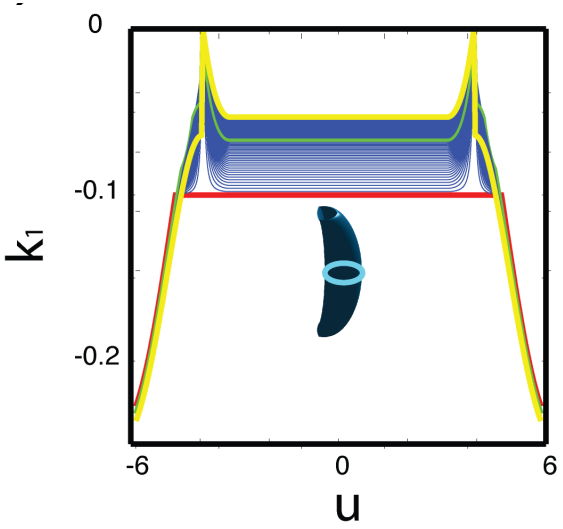

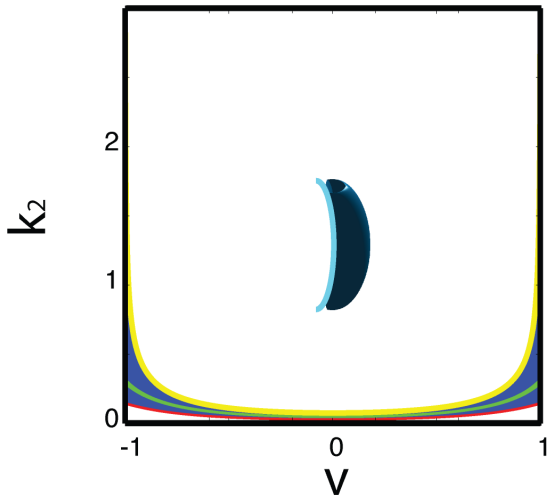

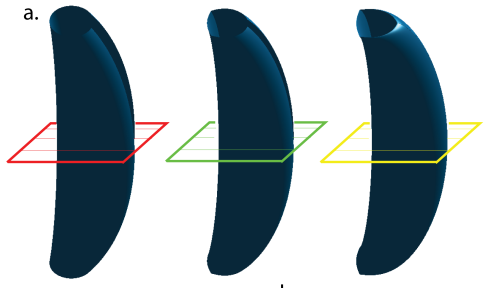

Pure bending energy

$$E_b = \int_u \int_v B\Big((\kappa_1 - \kappa_{10})^2 + 2\nu(\kappa_1 - \kappa_{10})(\kappa_2 - \kappa_{20}) + (\kappa_2 - \kappa_{20})^2\Big)\sqrt{EG - F^2}\,du\,dv$$

Phenomenological elastic fold energy (Plasticity is neglected)

$$E_f = \int_v B\frac{\sigma}{2}(\mathcal{N}^+ \cdot \mathcal{N}^- - 1)^2\sqrt{G}\,dv$$

(Bridson 2003, Dias 2011)

Total energy

$$E_{tot} = E_f + E_b$$

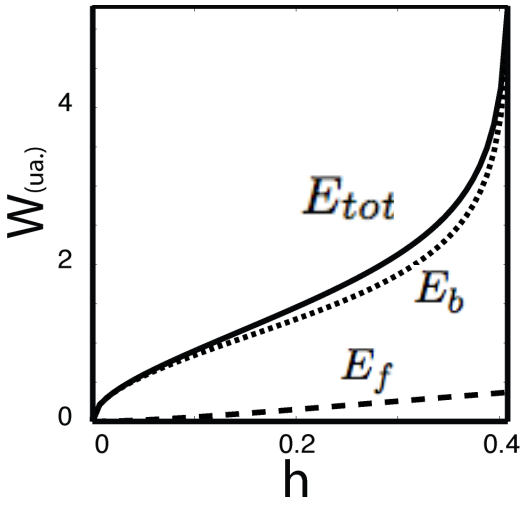

Divergence of k_2 at h_{max} and divergence of W

By shifting the fold into the positive gaussian curvature part of the banana similar opening system as the seedpod can be obtained

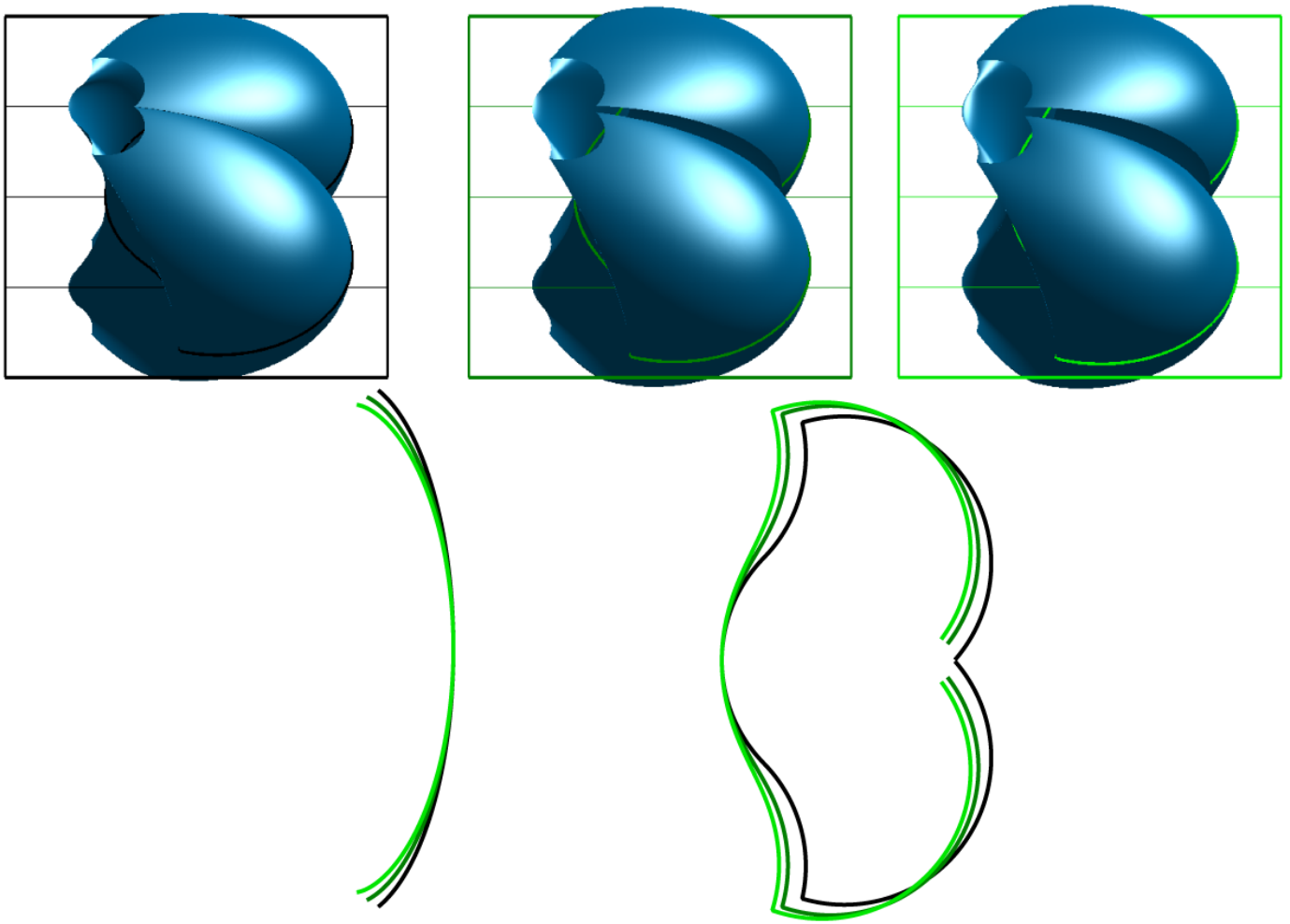

The narrower banana shell are the most efficient for opening

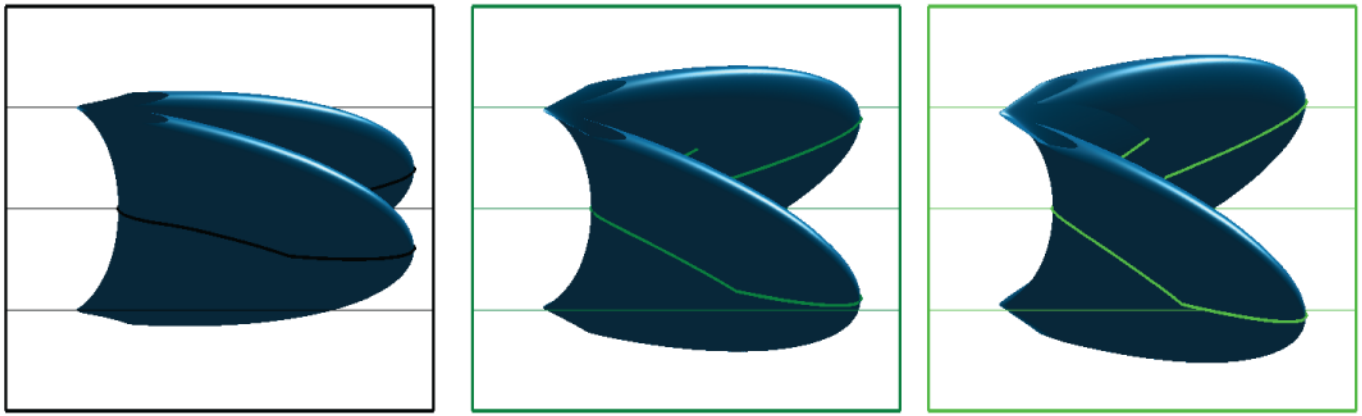

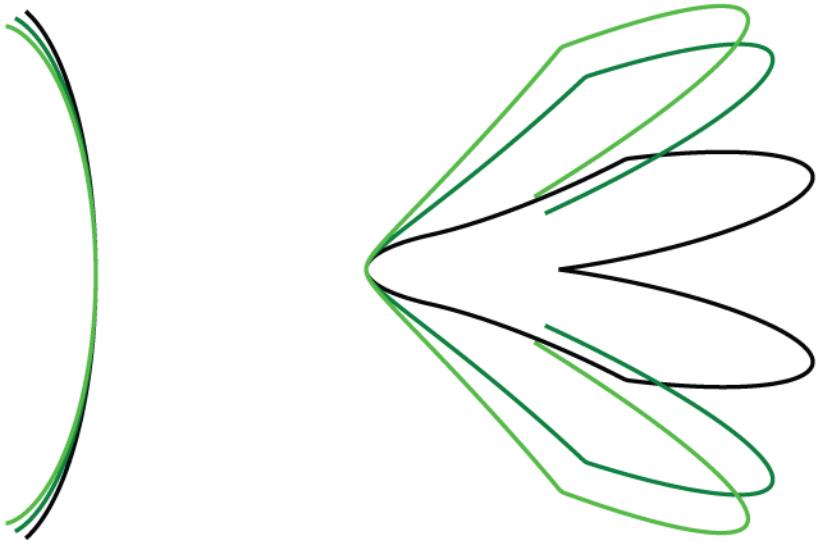

Conclusion

Modified Goursat surface to include stable folds:
Illustrated by the banana shaped family.
In revision at *Proc. Roy. Soc. A*

These exotic pure bending analytical solutions can be useful :

- To numericians for calibrating simulations with curved folds
- To designers for optimizing the shape and the ease of opening.

Interesting biomimetic thin shell converting an increase in longitudinal curvature into either a meridional closing or an opening.

Folding of open spherical shells inspired by pollen grain

E. Couturier[1], *E.Cerda*[1], *J.Dumais*[3], *E.Katifori*[2]

USACH Santiago, MSC Paris 7[1], *MPI*[2] *Göttingen*, *UAI*[3] *Viña − del − mar*

March 2, 2016

Pollen grain and isometric self-sealing

Turgid Dessicate

Lilium grandiflorum
2-fold symetry

Dianela caerula
3-fold symetry

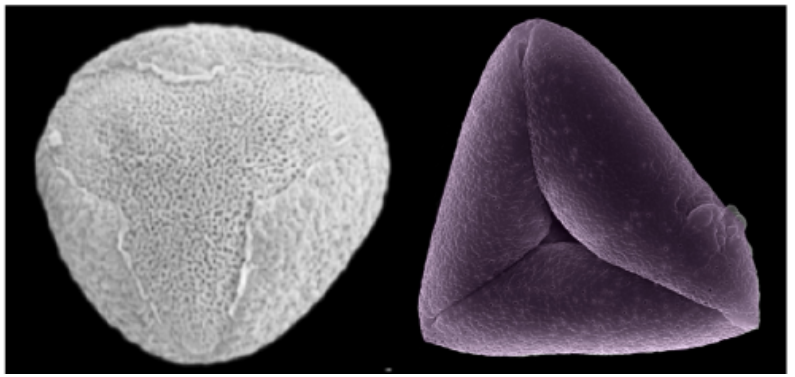

Thin shell.
(Thickness<Radius/10)

Isometric deformation.
Self- sealing.

(Katifori et al. 2010, Couturier et al. 2013)

Our model: a thin spherical shell with a n-fold rotationally symmetric aperture.

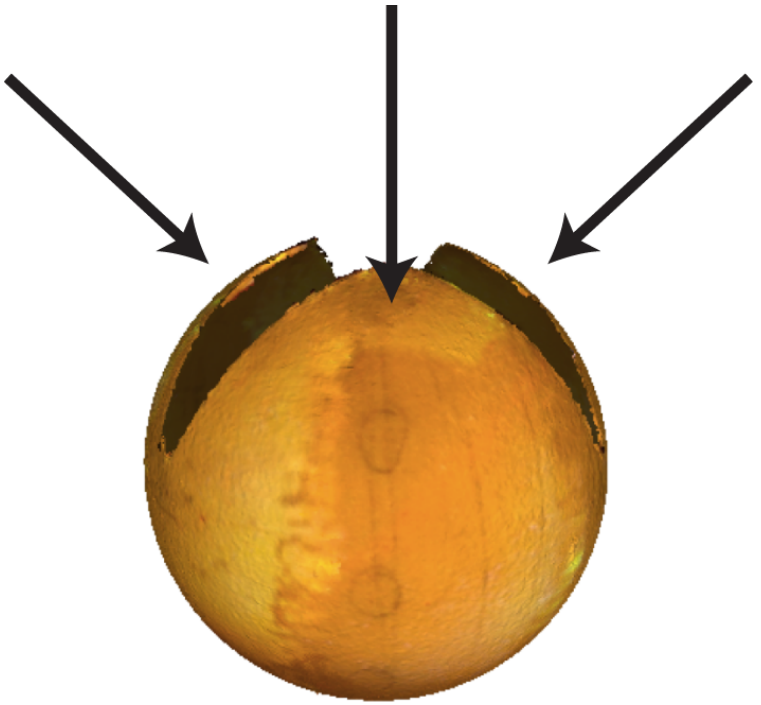

Isometric deformation of the sphere remains constant gaussian curvature surface.

A macroscopical model: a dissected ping-pong ball.

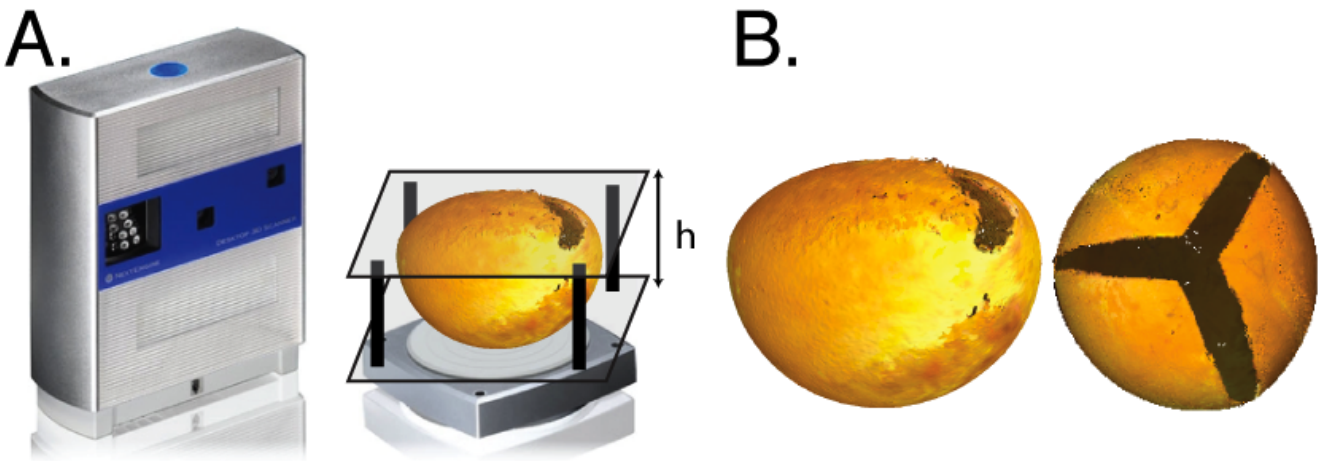

Isometric deformation using the tethered mesh method.

Eleni Katifori

Triggered by stitching the top extremities.
(Seung Nelson 1988, Katifori et al. 2010)

Isometric deformation using the tethered mesh method

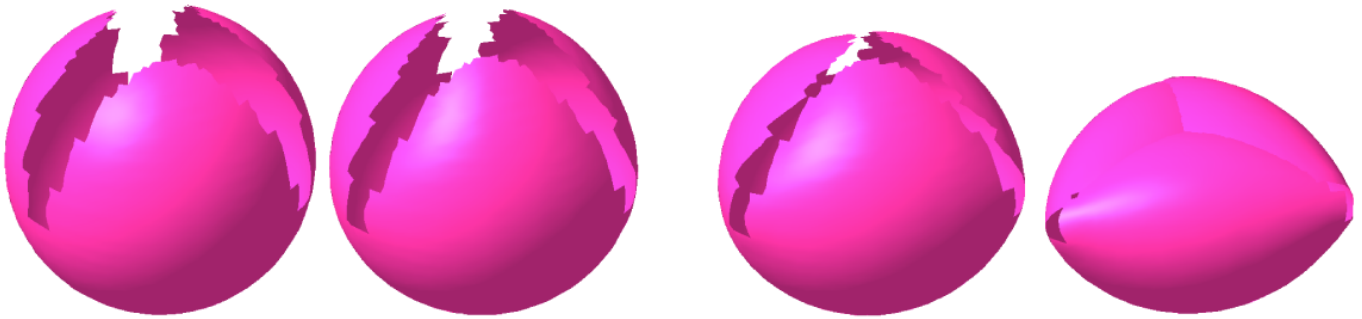

Triggered by repulsive lower corner.

The deformation is indeed isometric

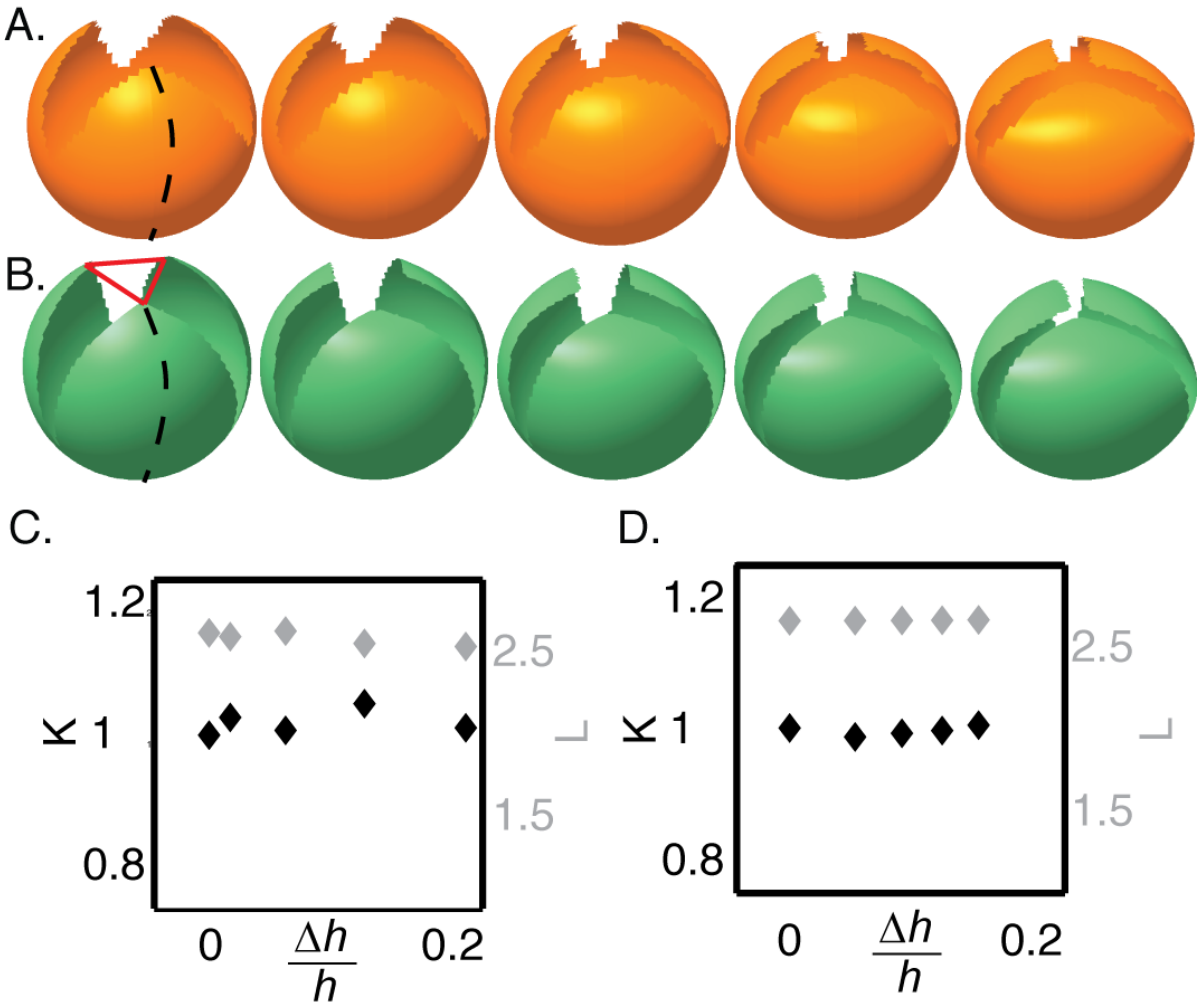

The first fundamental form

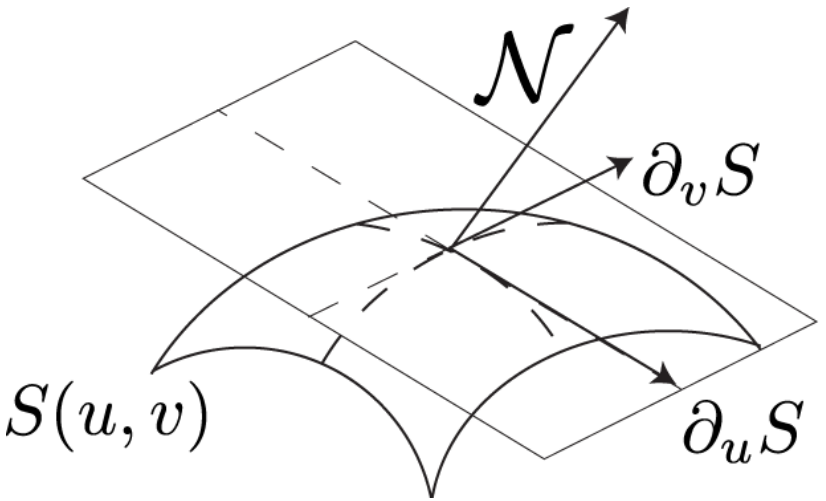

$$\mathrm{I}\begin{bmatrix} E &= (\partial_u S)^2 \\ F &= \partial_u S \cdot \partial_v S \\ G &= (\partial_v S)^2 \end{bmatrix}$$

The second fundamental form

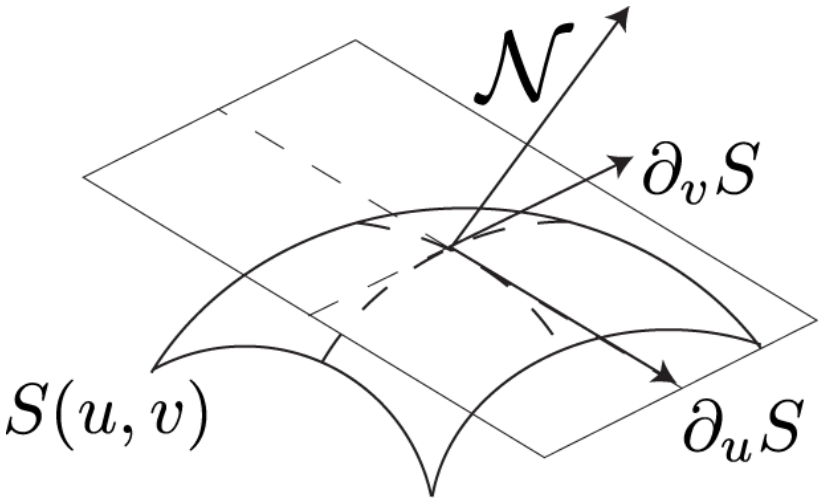

$$\mathrm{I}\begin{cases} E = (\partial_u S)^2 \\ F = \partial_u S \cdot \partial_v S \\ G = (\partial_v S)^2 \end{cases} \qquad \mathrm{II}\begin{cases} L = (\partial_{uu} S) \cdot \mathcal{N} \\ M = (\partial_{uv} S) \cdot \mathcal{N} \\ N = (\partial_{vv} S) \cdot \mathcal{N} \end{cases}$$

An alternative way to define a surface

$$\mathrm{I}\begin{bmatrix} E \\ F \\ G \end{bmatrix} \qquad \mathrm{II}\begin{bmatrix} L \\ M \\ N \end{bmatrix}$$

3 compatibility + equations. (Gauss-Codazzi)

System of ODE

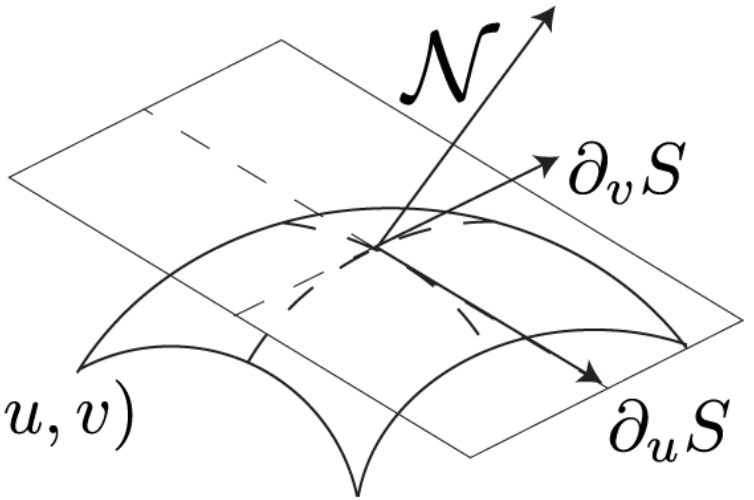

For one given surface, there is infinitely many way to write the fundamental forms.

An appropriate coordinate system to write the fundamental forms of a constant gaussian curvature surface with n –fold symmetry of rotation.

$$\begin{cases} E = -\frac{\lambda\rho^{n-2}\cos(n\theta)}{2} + \frac{e^{2\omega}+\lambda^2\rho^{2(n-2)}e^{-2\omega}}{4} \\ F = \frac{\lambda\rho^{n-1}\sin(n\theta)}{2} \\ G = \frac{\lambda\rho^{n}\cos(n\theta)}{2} + \frac{\rho^2(e^{2\omega}+\lambda^2\rho^{2(n-2)}e^{-2\omega})}{4} \\ L = e^{2\omega} - \lambda^2\rho^{2(n-2)}e^{-2\omega} \\ M = 0 \\ N = \rho^2(e^{2\omega} - \lambda^2\rho^{2(n-2)}e^{-2\omega}) \end{cases} \rightarrow \text{system of ODE} \rightarrow \text{Surface of constant gaussian curvature.}$$

(ρ, θ) are the coordinates. λ is a parameter. Only one equation of compatibility expressed with the function ω (Klotz 63).

$$\triangle\omega + e^{2\omega} - \lambda^2\rho^{2(n-2)}e^{-2\omega} = 0 \quad (1)$$

Case $\lambda = 0$: pde fully integrable.
Different parametrization of the sphere.

$$\begin{cases} E = -\cancel{\frac{\lambda\rho^{n-2}\cos(n\theta)}{2}} + \cancel{\frac{e^{2\omega}+\lambda^2\rho^{2(n-2)}e^{-2\omega}}{4}} \\ F = \cancel{\frac{\lambda\rho^{n-1}\sin(n\theta)}{2}} \\ G = \cancel{\frac{\lambda\rho^{n}\cos(n\theta)}{2}} + \cancel{\frac{\rho^2(e^{2\omega}+\lambda^2\rho^{2(n-2)}e^{-2\omega})}{4}} \\ L = e^{2\omega} - \cancel{\lambda^2\rho^{2(n-2)}e^{-2\omega}} \\ M = 0 \\ N = \rho^2(e^{2\omega} - \cancel{\lambda^2\rho^{2(n-2)}e^{-2\omega}}) \end{cases} \rightarrow \text{system of ODE} \rightarrow$$

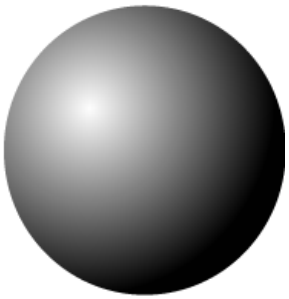

The pde is fully integrable:

$$\triangle\omega + e^{2\omega} = 0 \qquad (2)$$

Smyth surface: - ω invariant by rotation.
- Angular dependency in the fundamental forms

$$\begin{cases} E = -\frac{\lambda\rho^{n-2}\cos(n\theta)}{2} + \frac{e^{2\omega}+\lambda^2\rho^{2(n-2)}e^{-2\omega}}{4} \\ F = \frac{\lambda\rho^{n-1}\sin(n\theta)}{2} \\ G = \frac{\lambda\rho^{n}\cos(n\theta)}{2} + \frac{\rho^2(e^{2\omega}+\lambda^2\rho^{2(n-2)}e^{-2\omega})}{4} \\ L = e^{2\omega} - \lambda^2\rho^{2(n-2)}e^{-2\omega} \\ M = 0 \\ N = \rho^2(e^{2\omega} - \lambda^2\rho^{2(n-2)}e^{-2\omega}) \end{cases} \rightarrow \text{system of ODE} \rightarrow \text{Surface of constant gaussian curvature.}$$

The PDE becomes an ODE.

$$\partial_{\rho\rho}\omega + \frac{\partial_\rho\omega}{\rho} + e^{2\omega} - \lambda^2\rho^{2(n-2)}e^{-2\omega} = 0 \qquad (3)$$

Zoology of Smyth integrable CGC with a symmetry of rotation of order 3

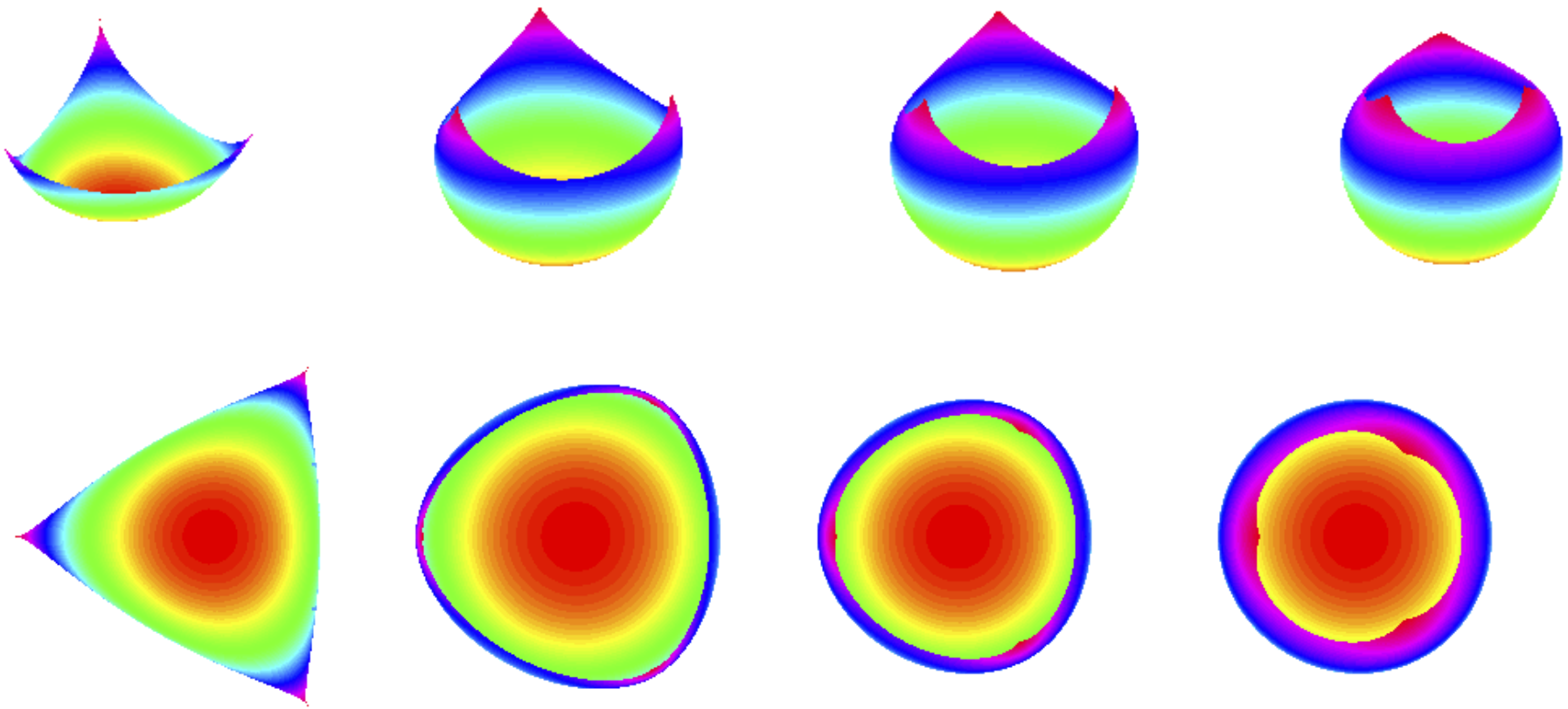

A one parameter family of surface.

ω_μ, a one-parameter family of solution of the compatibility equation of the sphere ($\lambda = 0$)

We choose the following one parameter family of function:

$$\omega_\mu = \log \frac{2\mu|(1 + (n-1)z^n)|}{|(1 - z^n)|^2 + \mu^2\rho^{2n}} \tag{4}$$

which are solution of the related equation:

$$\triangle\omega + e^{2\omega} = 0 \tag{5}$$

ω_μ is injected in the analytical expression of the fundamental form for $\lambda \neq 0$

$$
\begin{cases}
E = -\frac{\lambda \rho^{n-2} \cos(n\theta)}{2} + \frac{e^{2\omega} + \lambda^2 \rho^{2(n-2)} e^{-2\omega}}{4} \\
F = \frac{\lambda \rho^{n-1} \sin(n\theta)}{2} \\
G = \frac{\lambda \rho^{n} \cos(n\theta)}{2} + \frac{\rho^2 (e^{2\omega} + \lambda^2 \rho^{2(n-2)} e^{-2\omega})}{4} \\
L = e^{2\omega} - \lambda^2 \rho^{2(n-2)} e^{-2\omega} \\
M = 0 \\
N = \rho^2 (e^{2\omega} - \lambda^2 \rho^{2(n-2)} e^{-2\omega})
\end{cases}
\rightarrow \text{System of ODE integrated along } \rho \rightarrow \text{Mildly-varying gaussian curvature surface (MVGC)}
$$

ω_μ is injected in the analytical expression of the fundamental form for $\lambda \neq 0$

$$\begin{cases} E = -\frac{\lambda\rho^{n-2}\cos(n\theta)}{2} + \frac{e^{2\omega}+\lambda^2\rho^{2(n-2)}e^{-2\omega}}{4} \\ F = \frac{\lambda\rho^{n-1}\sin(n\theta)}{2} \\ G = \frac{\lambda\rho^{n}\cos(n\theta)}{2} + \frac{\rho^2(e^{2\omega}+\lambda^2\rho^{2(n-2)}e^{-2\omega})}{4} \\ L = e^{2\omega} - \lambda^2\rho^{2(n-2)}e^{-2\omega} \\ M = 0 \\ N = \rho^2(e^{2\omega} - \lambda^2\rho^{2(n-2)}e^{-2\omega}) \end{cases}$$

→ System of ODE integrated along ρ → Mildly-varying gaussian curvature surface (MVGC)

$$\triangle\omega + e^{2\omega} - \lambda^2\rho^{2(n-2)}e^{-2\omega} = -\lambda^2\rho^{2(n-2)}e^{-2\omega} \neq 0$$

The coefficient of the fundamental forms of the surface are different from F,G,L,M,N.

A two-parameters family of surface of mildly-varying gaussian curvature (MVCG)

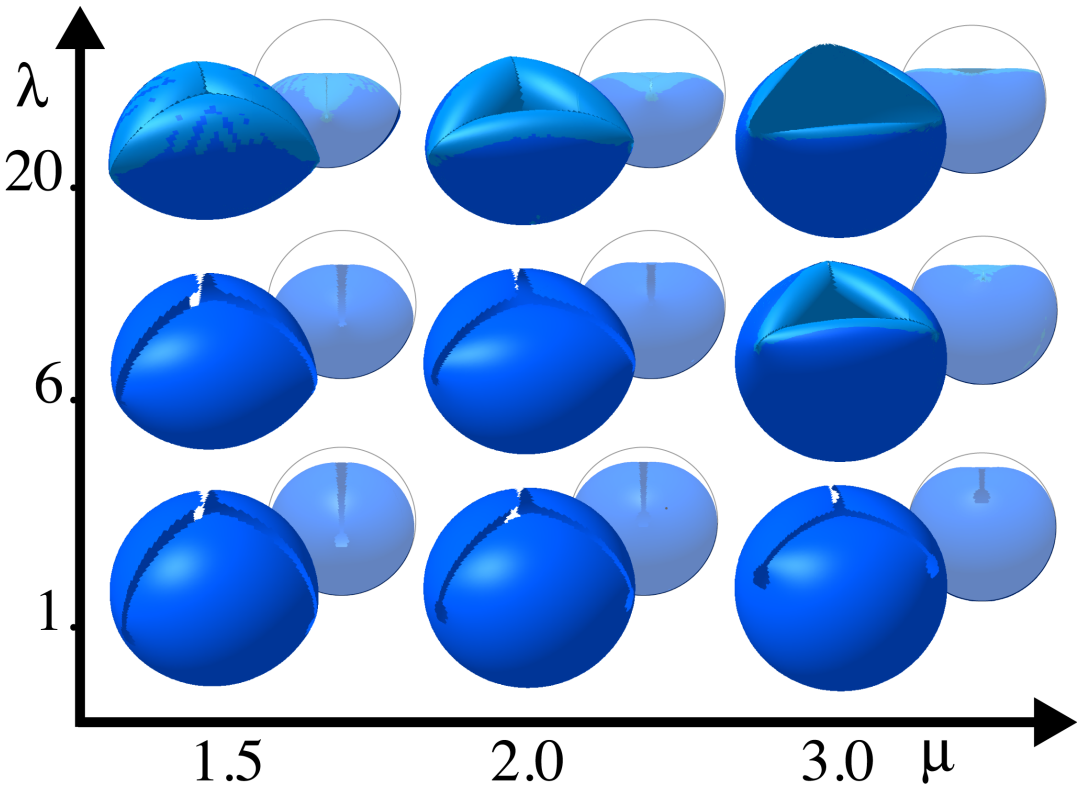

The gaussian curvature does not vary more than 5% up to diminution of the top the surface of 25%

Mildly-varying constant gaussian curvature for symmetry of higher order.

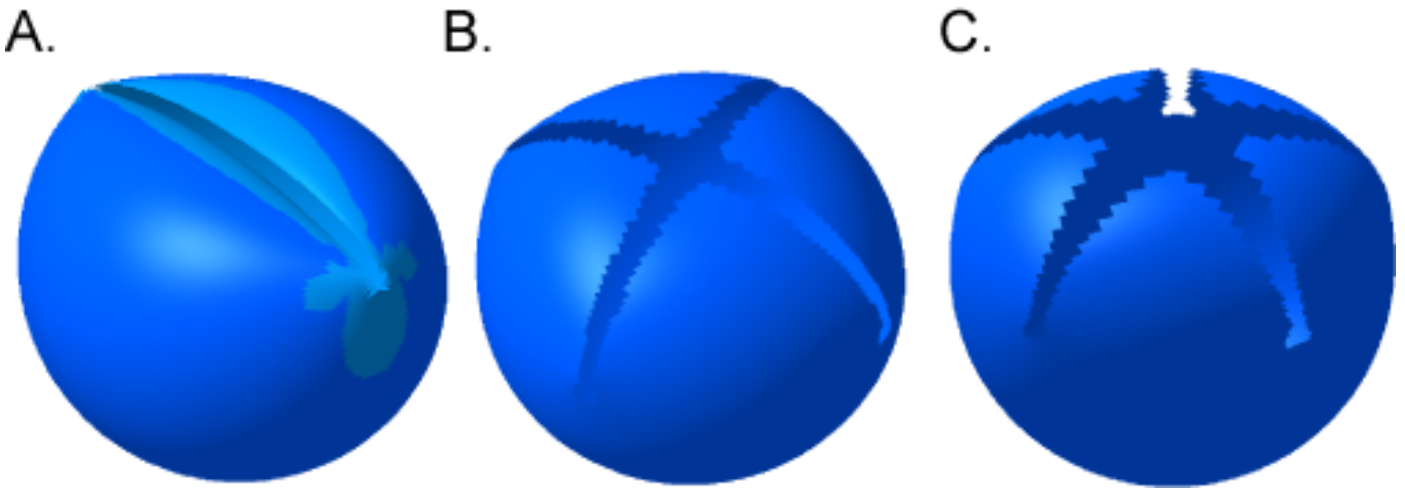

Best Fit inferior to 1 % of the diameter for simulations triggered by stitching the top extremities (N=9)

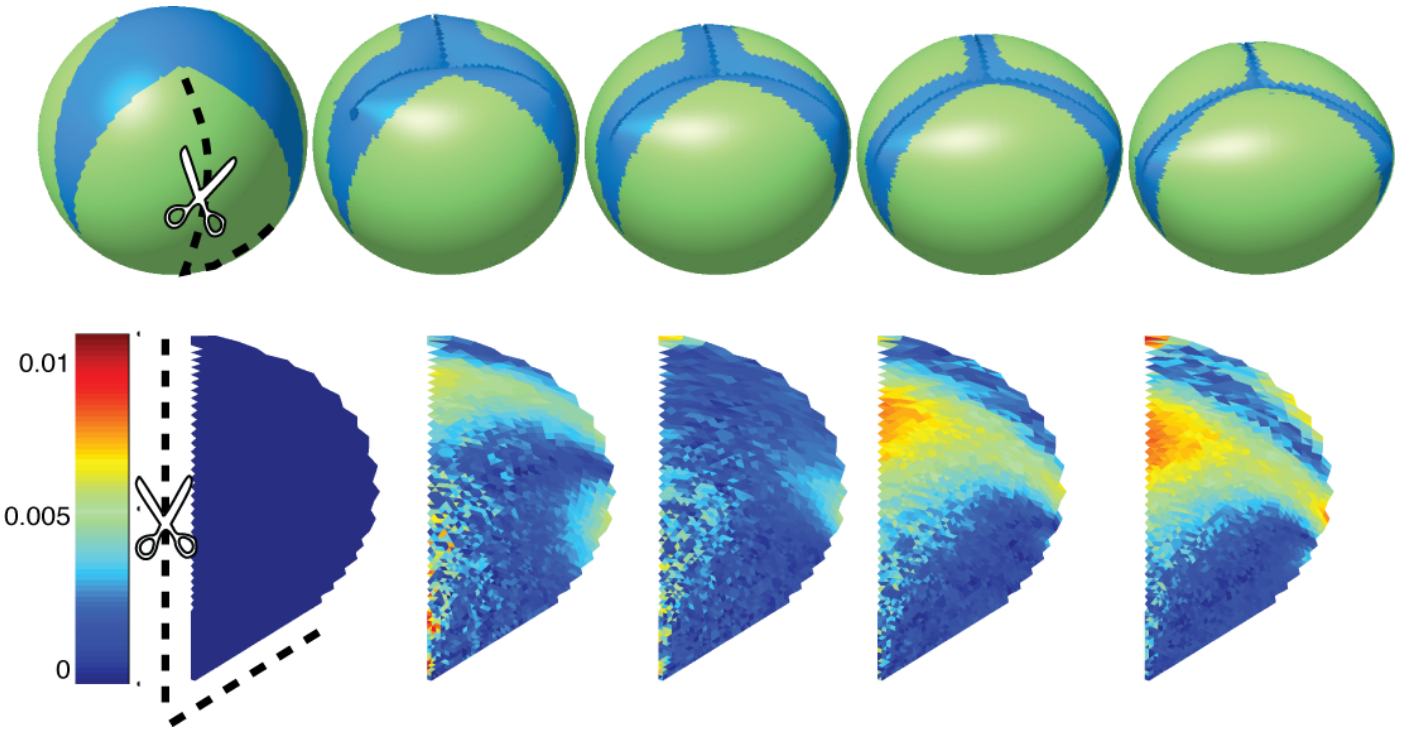

Best Fit inferior to 1 % of the diameter for simulations triggered by stitching the top extremities (N=9)

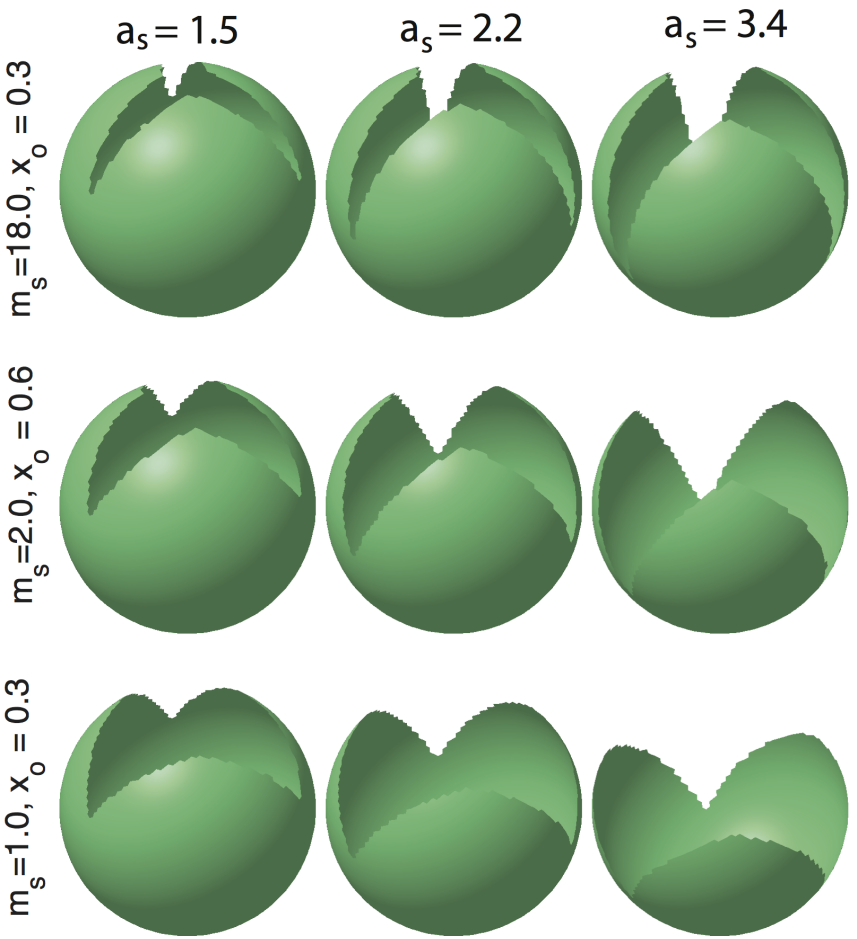

Best Fit inferior to 2 % of the diameter for the experiment (N=1)

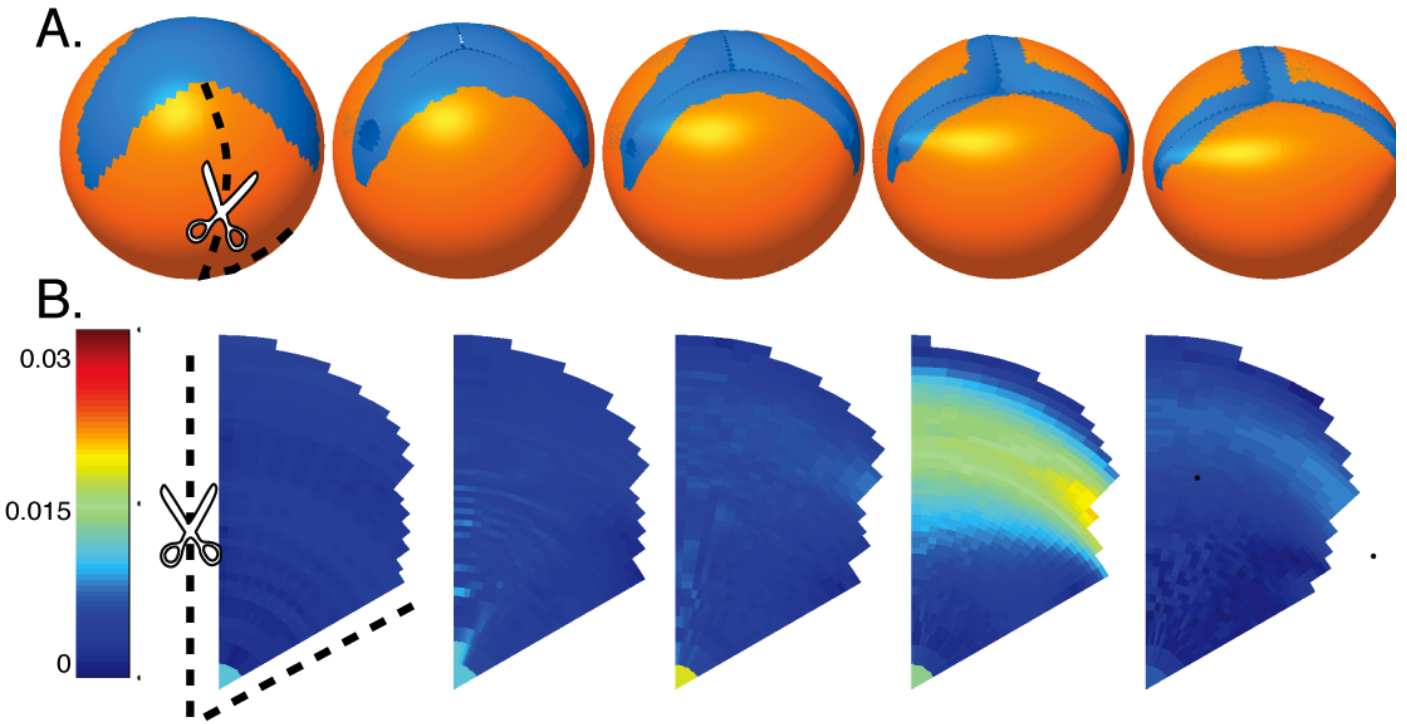

Section in the plane of symmetry.

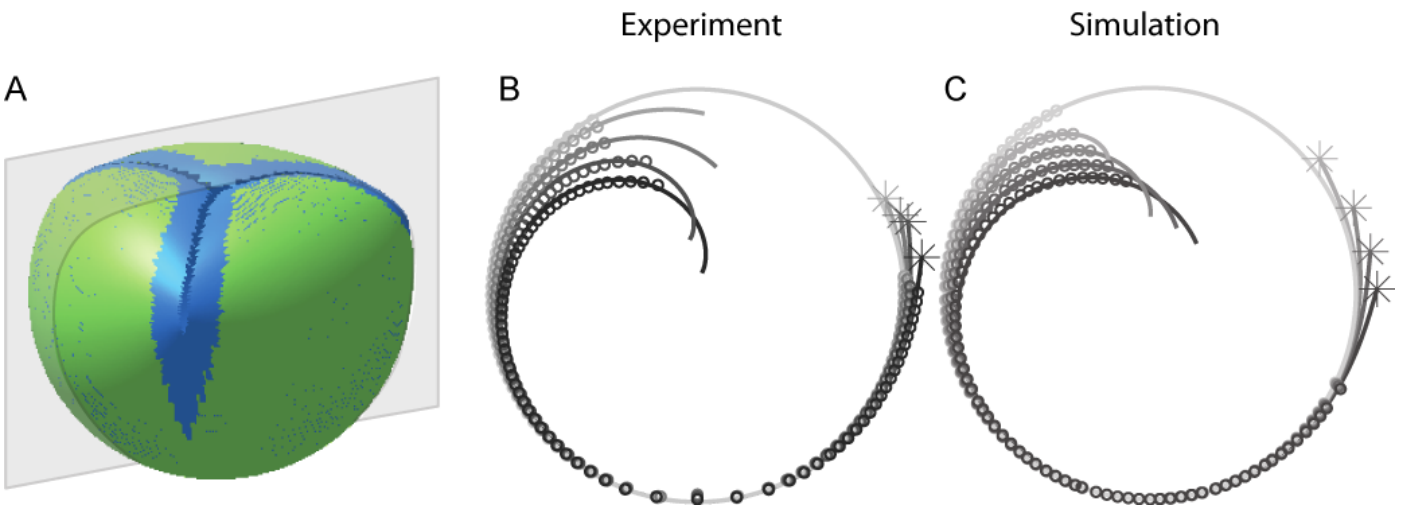

Very good quality of the fit.
Close analytic formula for the line in the plane of symmetry.

The singularity of the MVCG surface gets closer to the thin shell when the load increases.

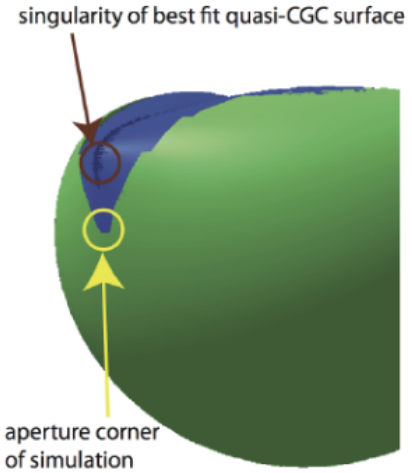

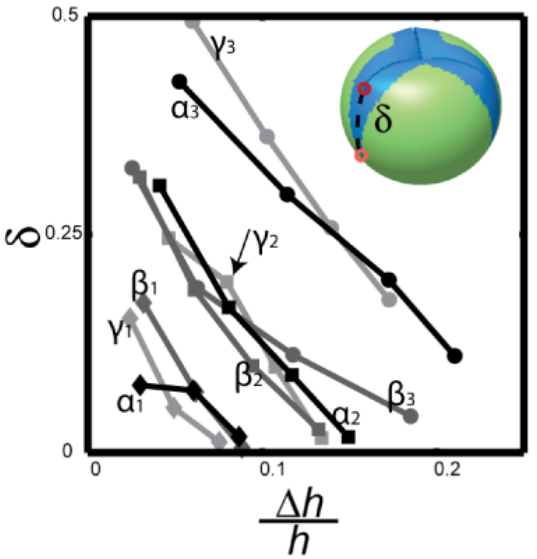

Isometric deformation using the tethered mesh method

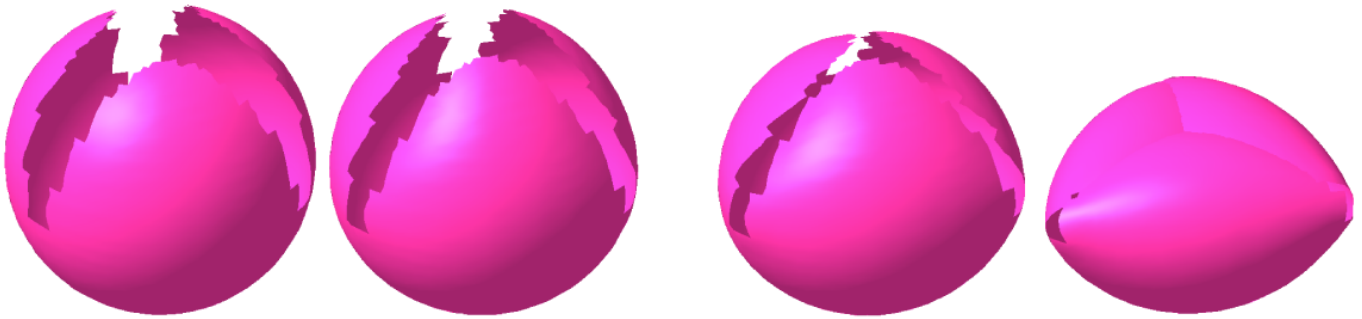

Triggered by repulsive lower corner.

Surface derived from other solution of the Liouville equation

$$\triangle\omega + e^{2\omega} = 0 \tag{6}$$

The general solution of the Liouville equation is:

$$\omega = \log \frac{2|P_z|}{1+|P|^2} \tag{7}$$

$P = \frac{\mu z}{(1+az^n+bz^{2n})^2}$,

Shape that can be obtained for various P

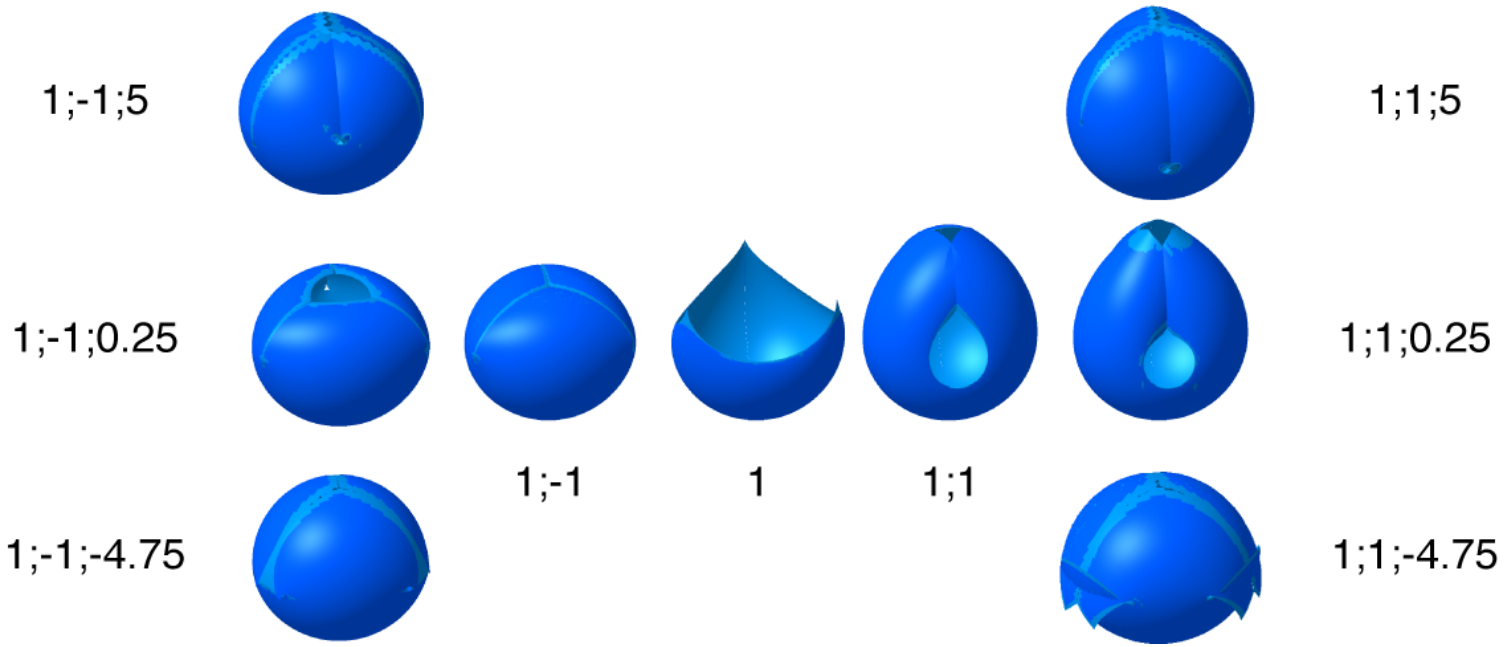

Isometric deformation using the tethered mesh method

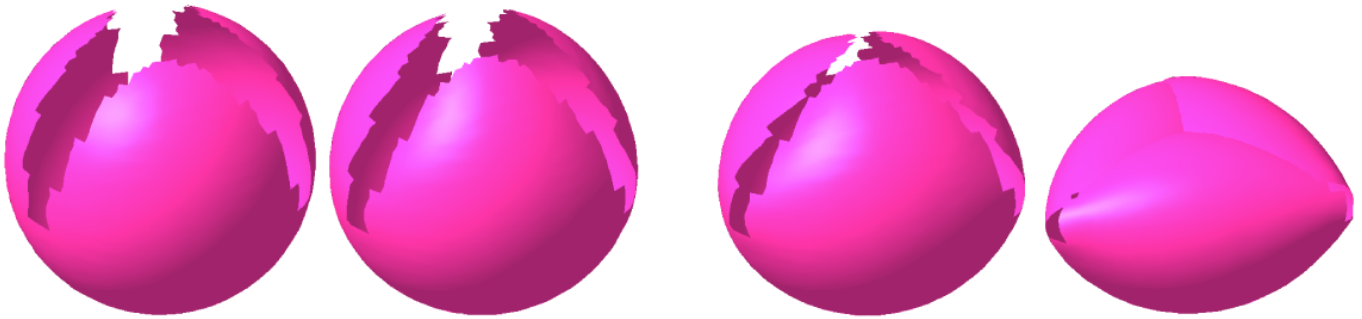

Triggered by repulsive lower corner.

Surface derived from other solution of the Liouville equation

$$\triangle\omega + e^{2\omega} = 0 \tag{8}$$

The general solution of the Liouville equation is:

$$\omega = \log \frac{2|P_z|}{1+|P|^2} \tag{9}$$

- Closing $P = \frac{\mu z}{(1-z^n)^2}$,
- Opening $P = \frac{\mu z}{(1+z^n)^2}$

Mode of opening by repulsive tips

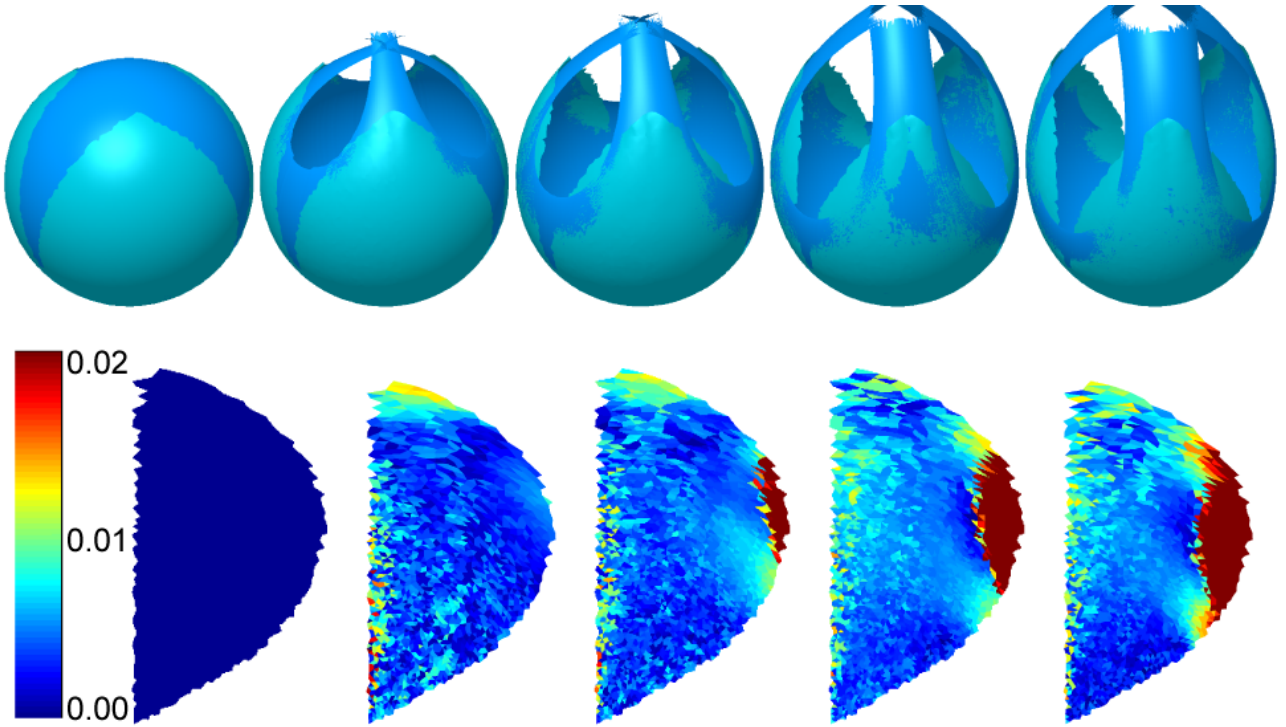

Numerical experimentation inspired by pollen grains

- **An integrable family of surface remarkably close of two modes of deformation of a shell with a dissected top:**
  - Deformation induced by joining the tips (complete surface) (N= 9).
  - Deformation induced by compression between two plates (lack some part of the edges) (N=1).
- **When the load increases, the singularity of the MVCG surface gets closer to the real surface.**

(Couturier et al. 2013)

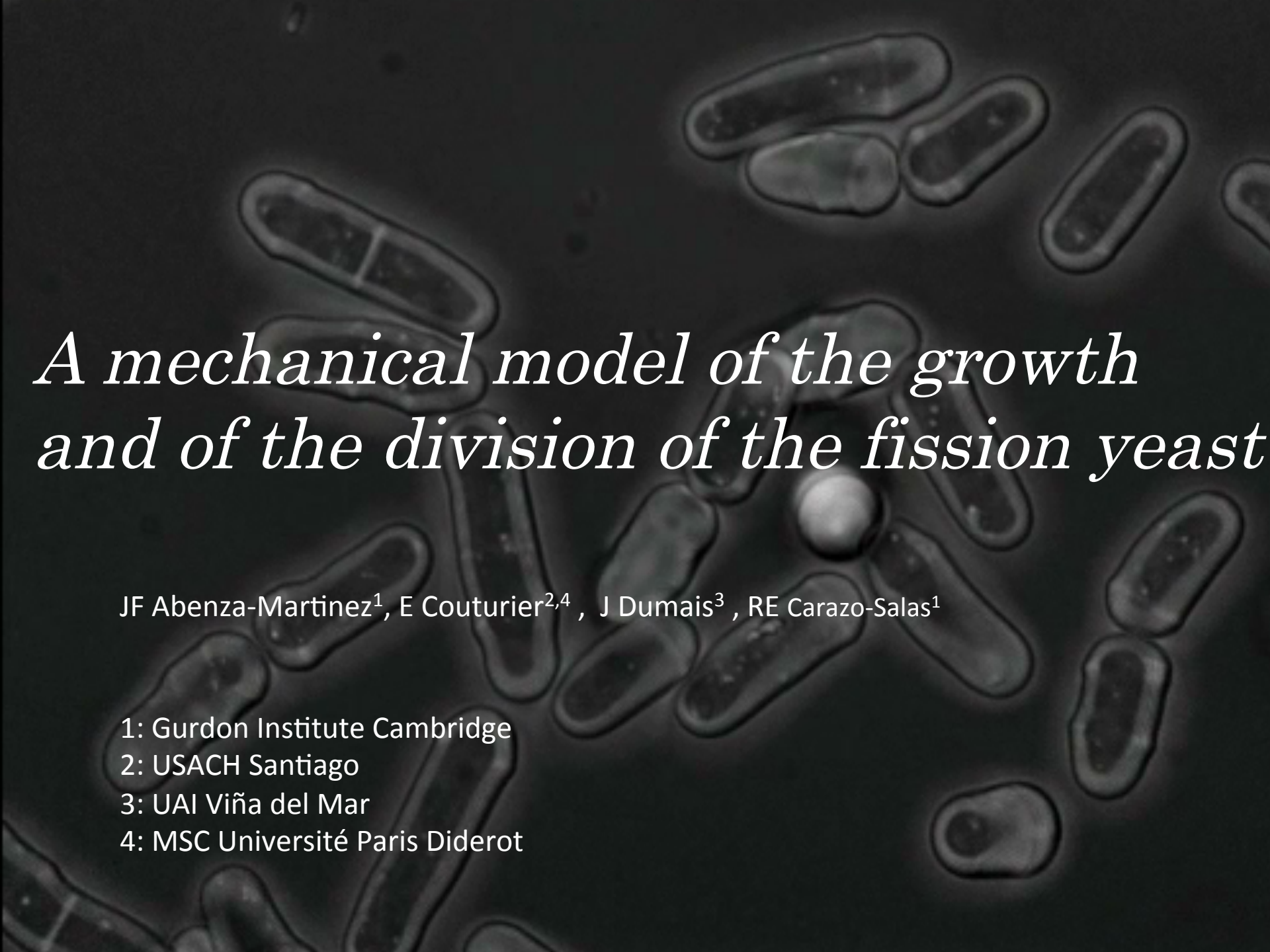

A mechanical model of the growth and of the division of the fission yeast

JF Abenza-Martinez[1], E Couturier[2,4] , J Dumais[3] , RE Carazo-Salas[1]

1: Gurdon Institute Cambridge
2: USACH Santiago
3: UAI Viña del Mar
4: MSC Université Paris Diderot

The fission yeast

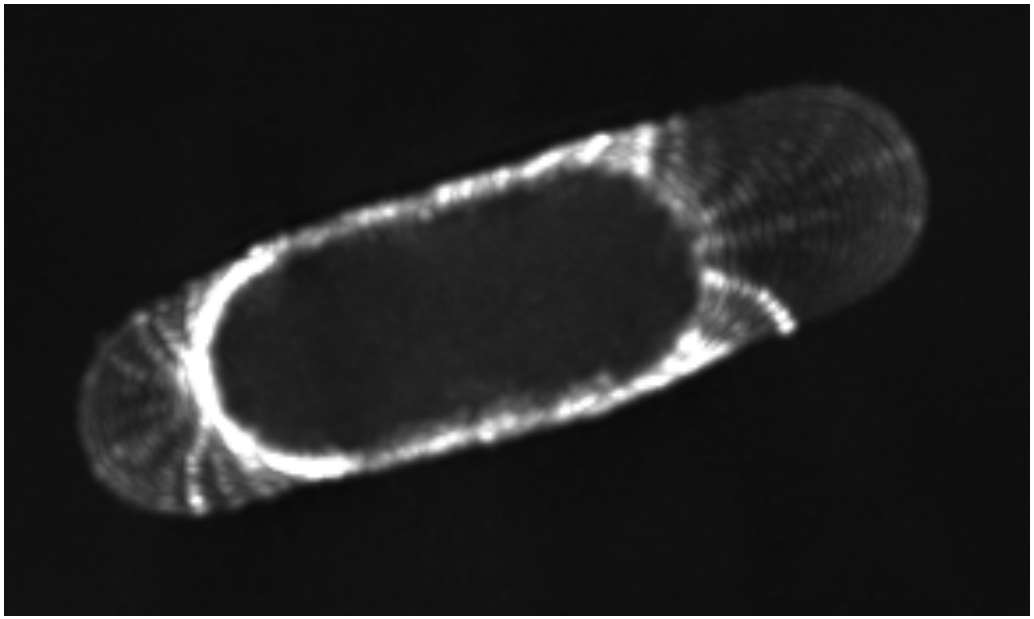

Radius: 2 μm
Cell wall thickness: 0.2 μm (Minc et al. 2009)
Tip growth

Wall Elasticity in Fission Yeast

turgid

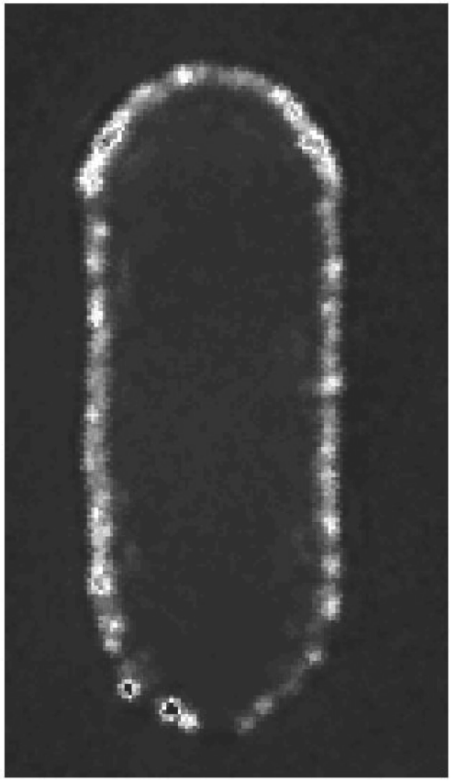

plasmolyzed

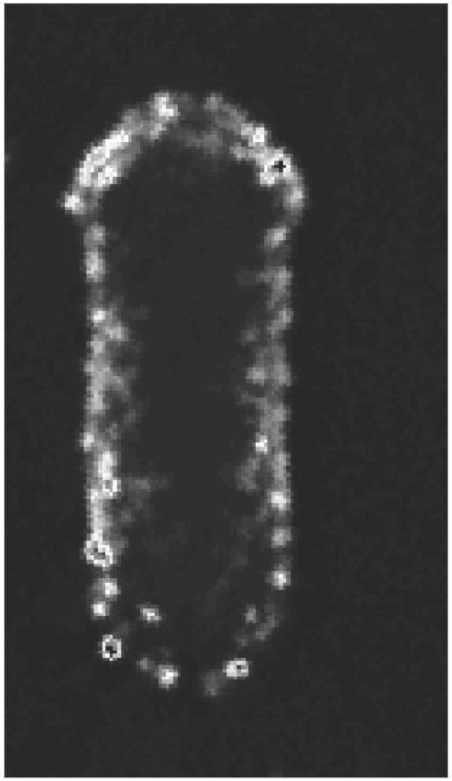

Wall Elasticity in Fission Yeast

turgid

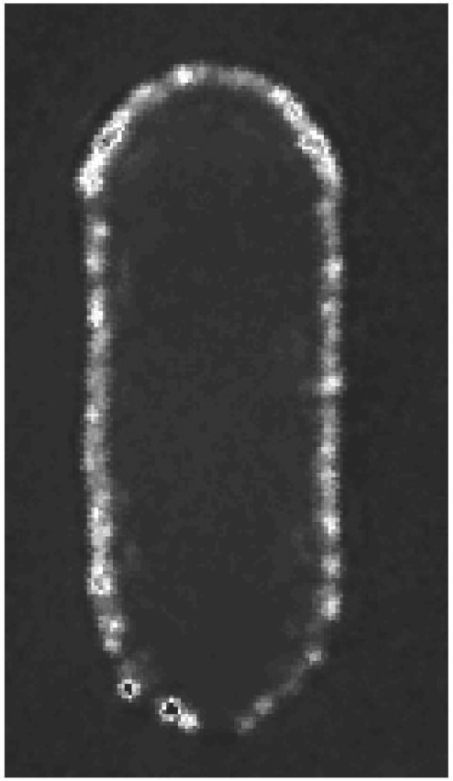

plasmolyzed

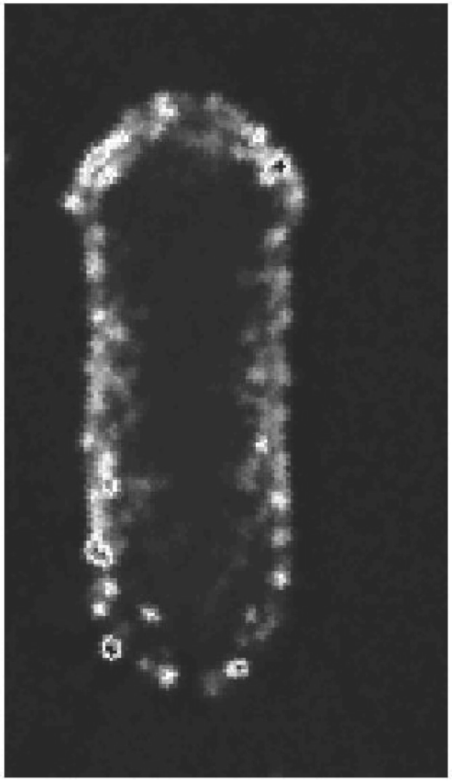

Strain in the cylindrical part of the cell wall.
Longitudinal: 13 ± 0.5 % (N=38)
Meridional: 24 ± 0.5 % (N=38)

The pressure in the cell is the motor of the growth. (Minc et al. 2009)

Pollen tube

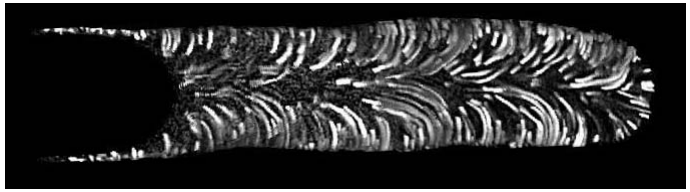

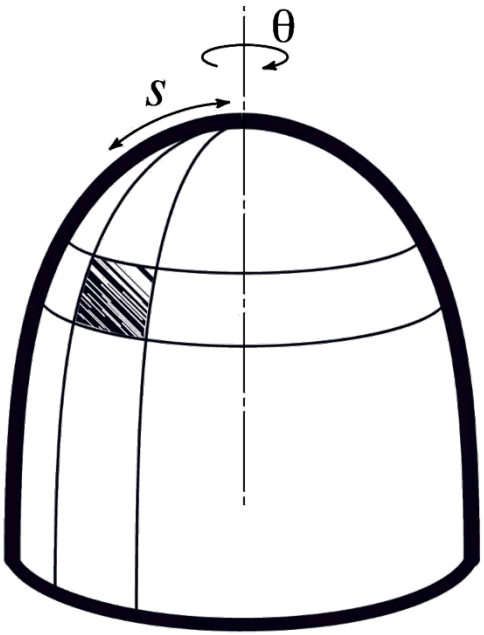

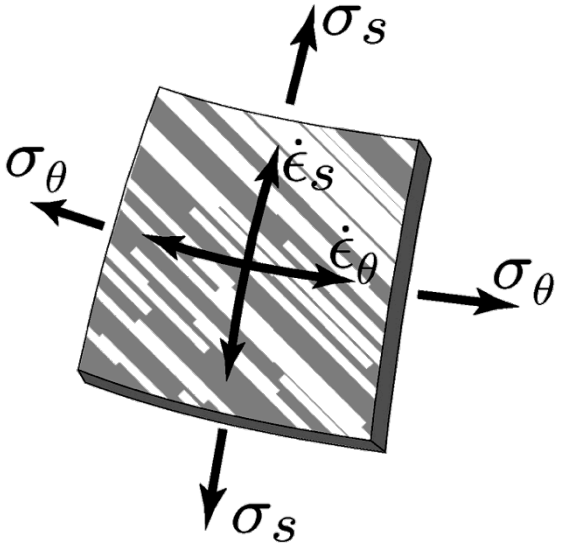

Pollen tube

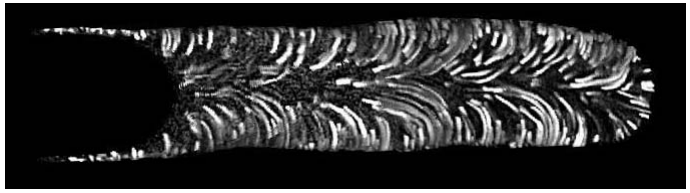

Growth anisotropy = Elastic strain anisotropy

Rojas 2011

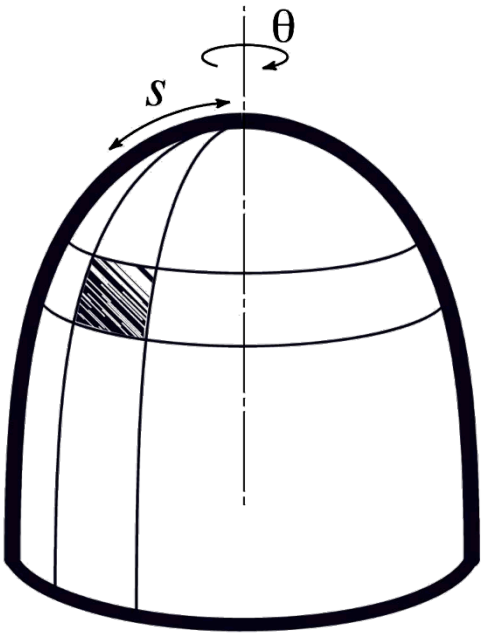

Pollen tube

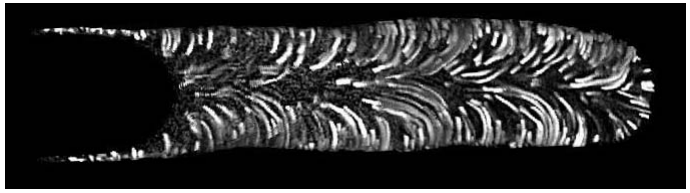

Growth anisotropy = Elastic strain anisotropy

Rojas 2011

$$\dot{\varepsilon} = k[C^*]\varepsilon$$

Wall chemistry
(rate of incorporation)

Wall mechanics
(elastic strain)

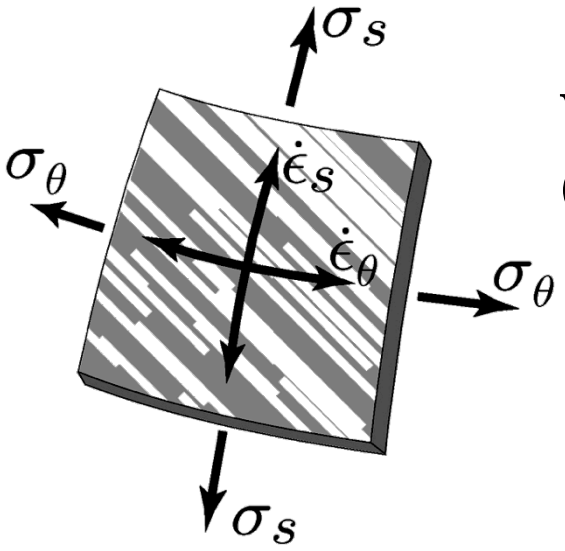

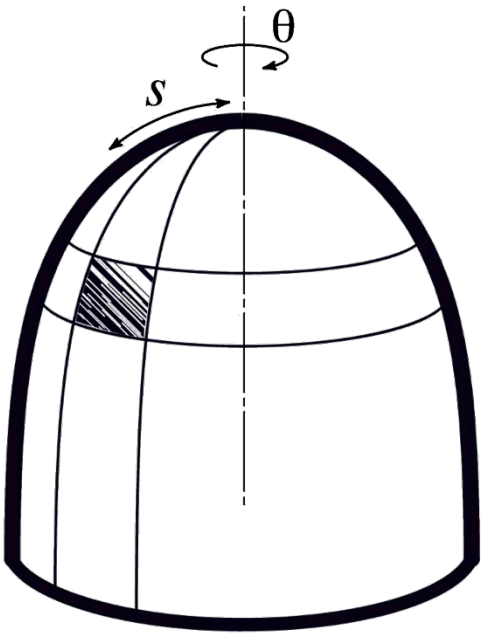

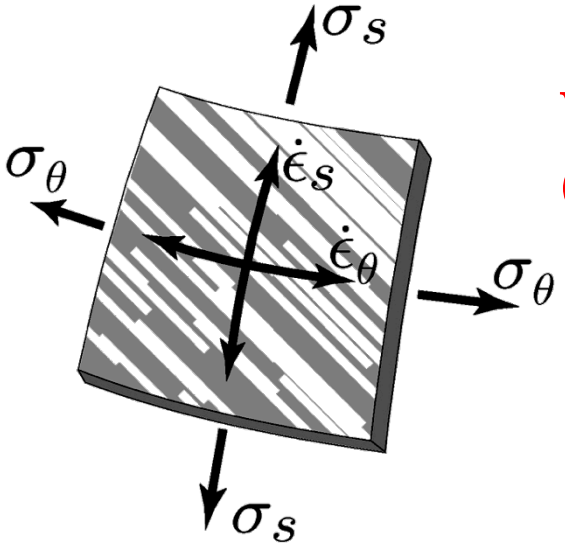

Pollen tube

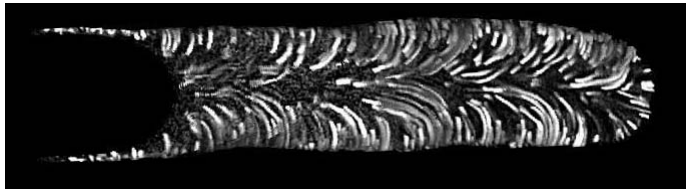

Growth anisotropy = Elastic strain anisotropy

Rojas 2011

$$\dot{\varepsilon} = k[C^*]\varepsilon$$

Wall chemistry (rate of incorporation)

Wall mechanics (elastic strain)

What sets the rate of cell expansion?

Fission yeast

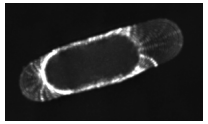

Polarly Distributed Factors

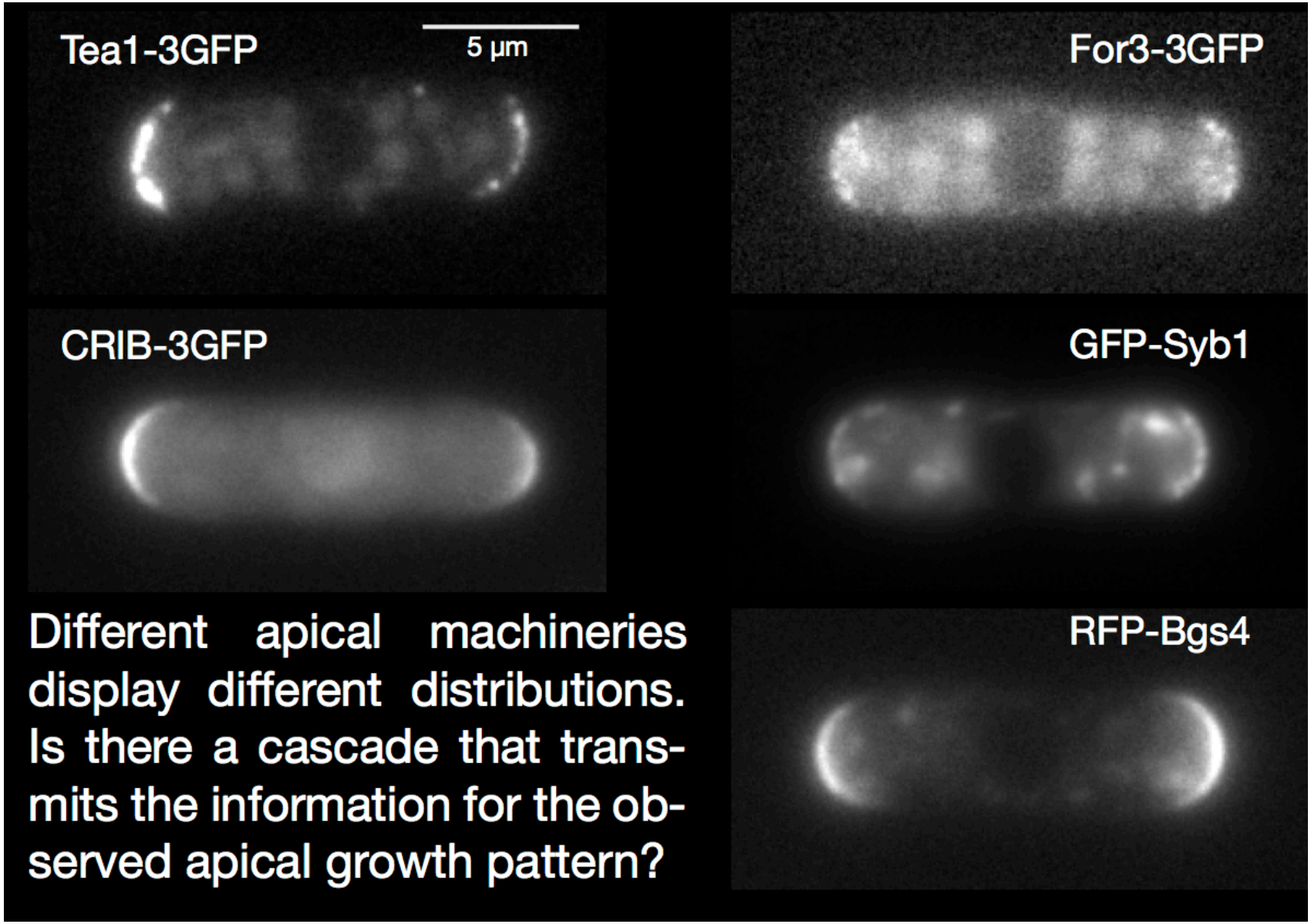

Different apical machineries display different distributions. Is there a cascade that transmits the information for the observed apical growth pattern?

A first model of the fission yeast growth

Membrane model

Indirect estimation of the elastic strains using the contour

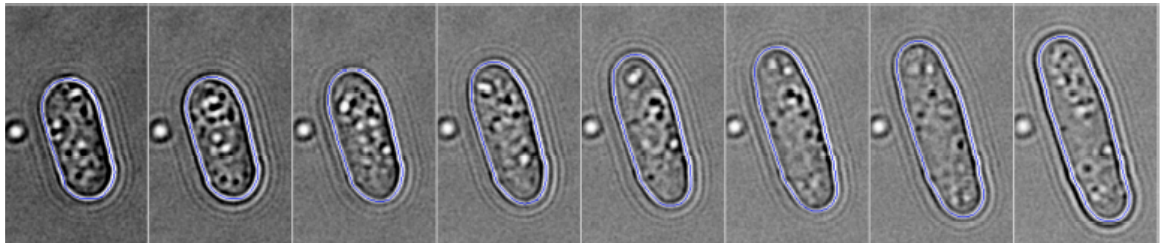

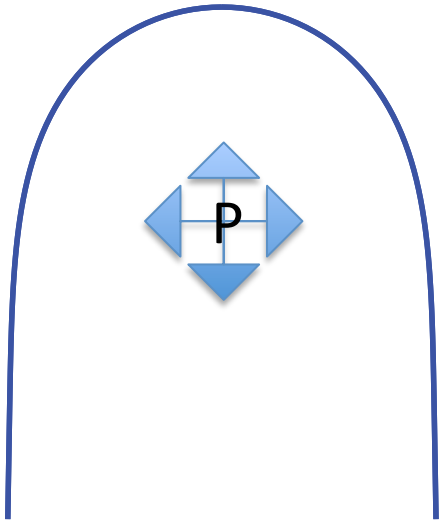

Contour

↓

Elastic strain

ε

A first model of the fission yeast growth

Membrane model

Indirect estimation of the elastic strains using the contour

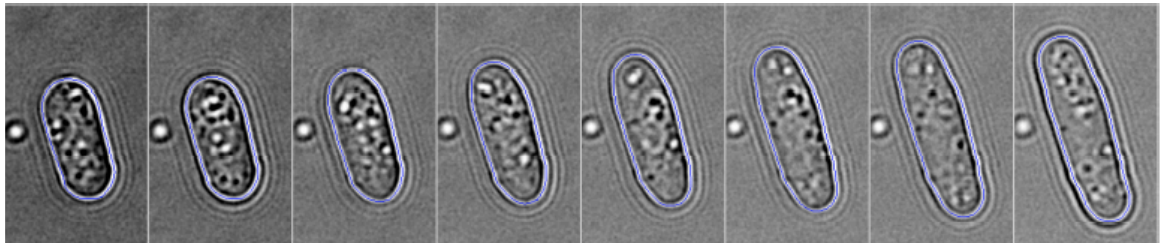

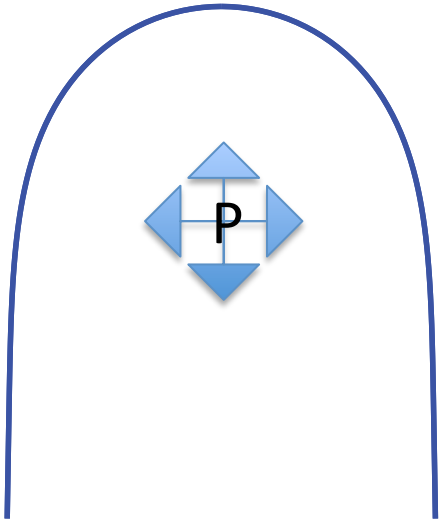

Contour

↓

Elastic strain

$$\dot{\varepsilon} = k[C^*]\varepsilon$$

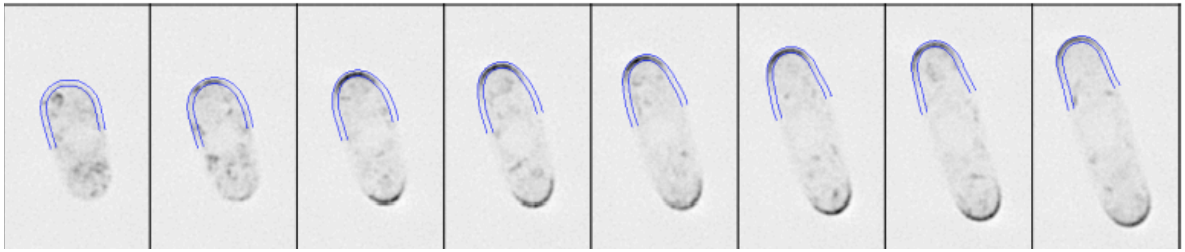

Fluorescent profile of a protein

A first model of the fission yeast growth

Membrane model

Indirect estimation of the elastic strains using the contour

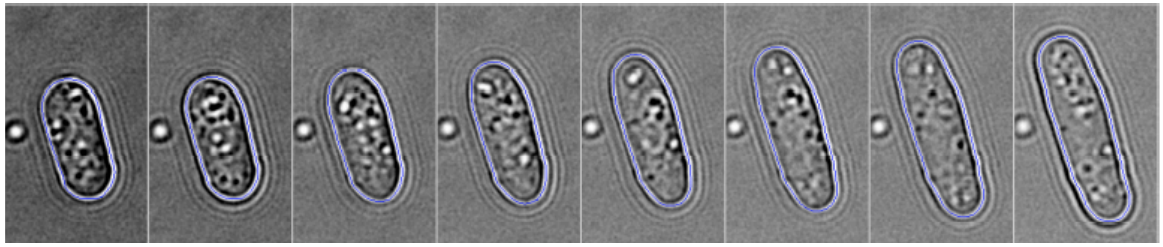

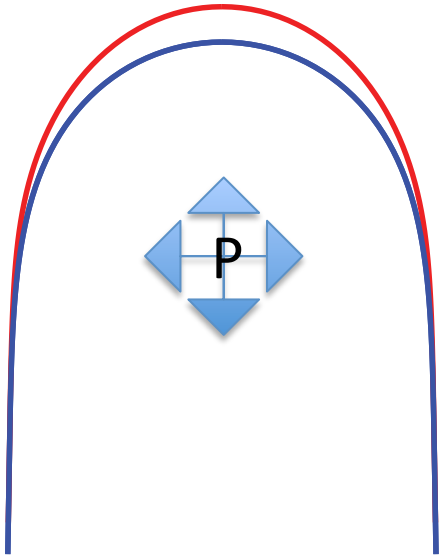

Contour

↓

Elastic strain

$$\dot{\varepsilon} = k[C^*]\varepsilon$$

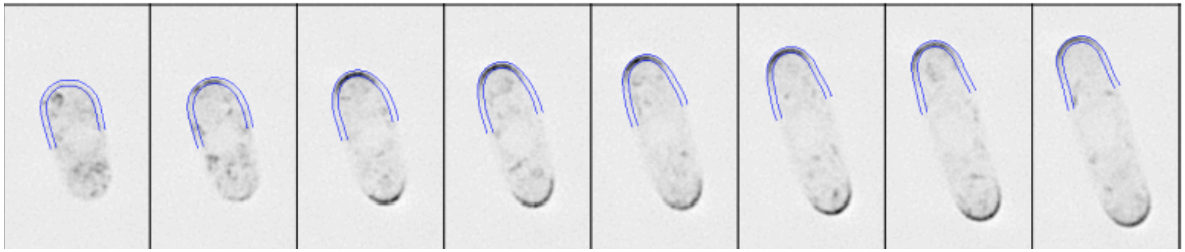

Fluorescent profile of a protein

A second model of the fission yeast growth

Direct estimation of the strain in the cell wall using plasmolysis experiments.

plasmolyzed

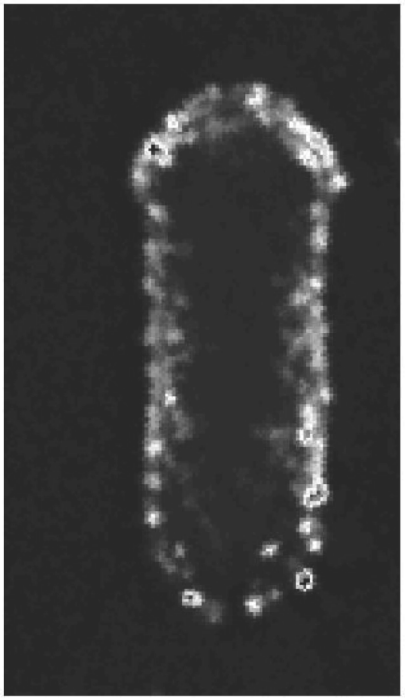

turgid

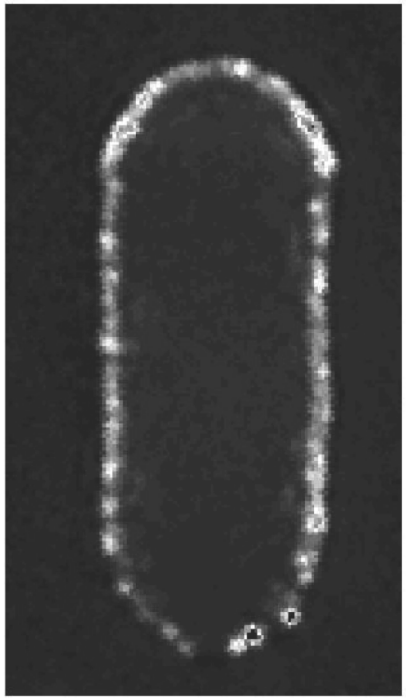

A second model of the fission yeast growth

Direct estimation of the strain in the cell wall using plasmolysis experiments.

Axisymmetric thin shell
under pressure.
Reissner 1950.
Taber 1988.

Linear material.
Bending.
Transverse shear.

plasmolyzed

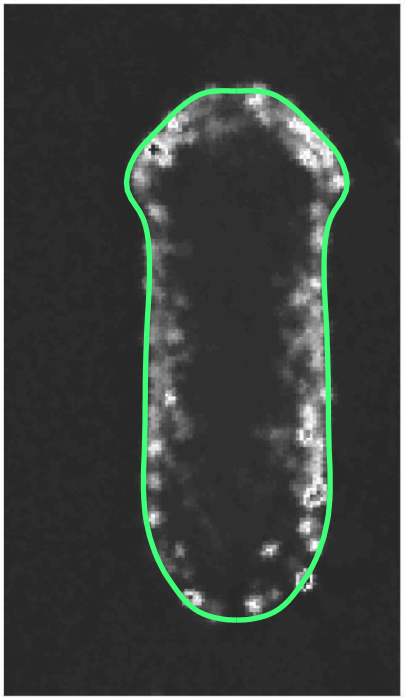

turgid

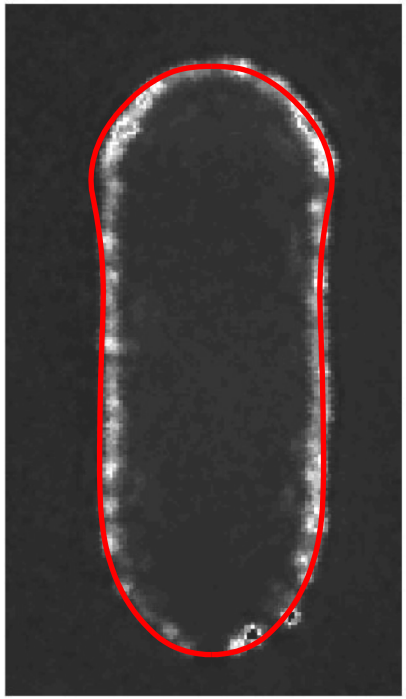

A second model of the fission yeast growth

Direct estimation of the strain in the cell wall using plasmolysis experiments.

plasmolyzed

turgid

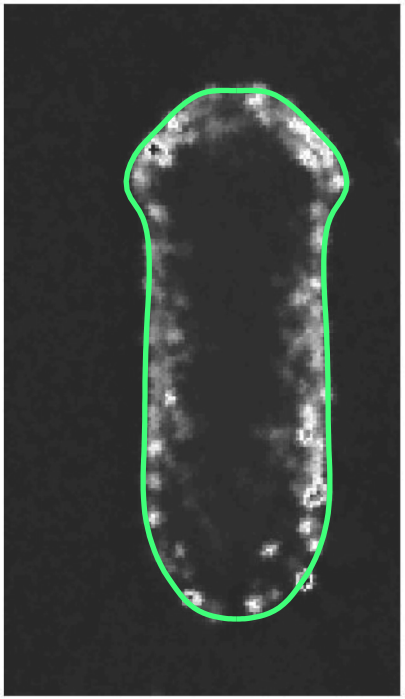

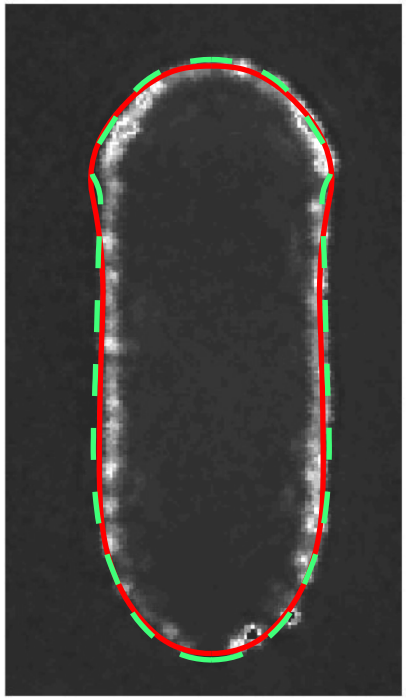

Axisymmetric thin shell
under pressure.
Reissner 1950.
Taber 1988.

Linear material.
Bending.
Transverse shear.

P/E= 0.018 ± 0.0008 (N = 24)

ν=0.033 ± 0.005 (N = 24)

Coherent with direct measurement
Longitudinal strain / Meridional strain = 0.54 (N=33)

Initial step of the growth

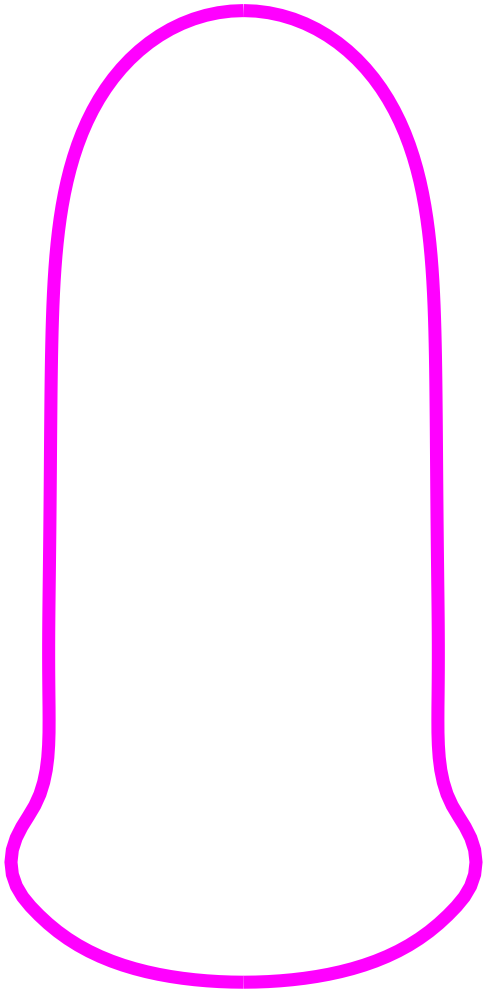

Typical contour of a plamolyzed cell at mechanical rest

Swelling

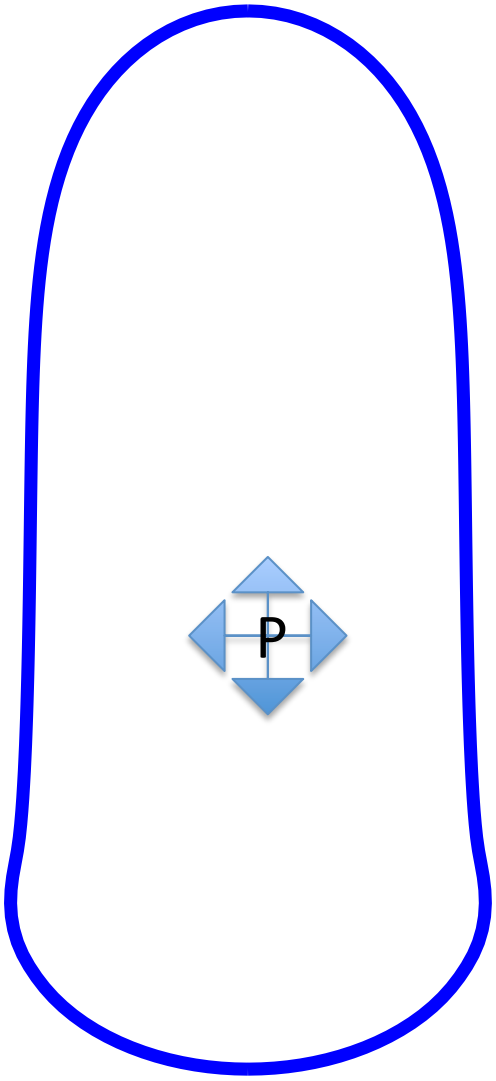

Direct estimation of the strains

Modification of the energy to include polar growth

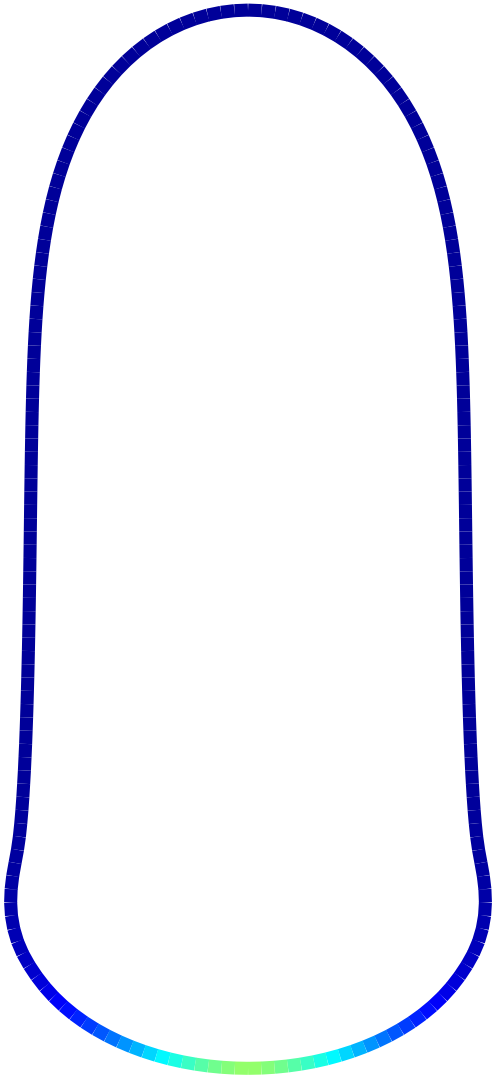

Direct estimation of the strains

Modification of the energy to include growth

$$w(\lambda_{11}\lambda_{11}^*, \lambda_{22}\lambda_{22}^*, \gamma_2, \kappa_{11}, \kappa_{22})$$

$$\lambda_{11}^* = \frac{1}{1+\delta(\lambda_{11}^0 - 1)k[C^*]}$$
$$\lambda_{22}^* = \frac{1}{1+\delta(\lambda_{22}^0 - 1)k[C^*]}$$

Modification of the energy to include polar growth

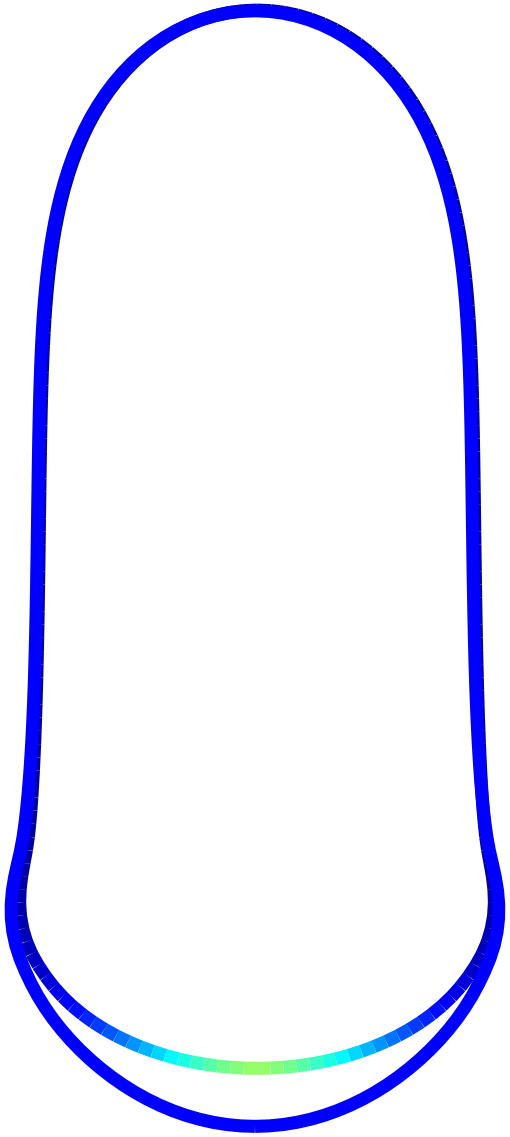

Direct estimation of the strains

Modification of the energy to include growth

$$w(\lambda_{11}\lambda_{11}^{*}, \lambda_{22}\lambda_{22}^{*}, \gamma_2, \kappa_{11}, \kappa_{22})$$

$$\lambda_{11}^{*} = \frac{1}{1+\delta(\lambda_{11}^{0}-1)k[C^{*}]}$$
$$\lambda_{22}^{*} = \frac{1}{1+\delta(\lambda_{22}^{0}-1)k[C^{*}]}$$

Bgs4

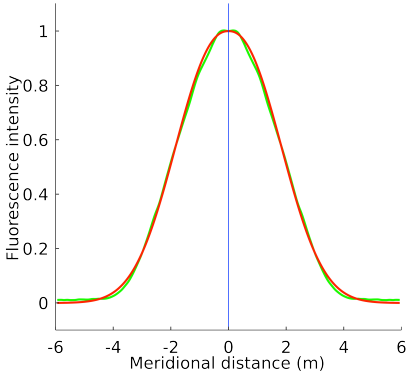

CRIB

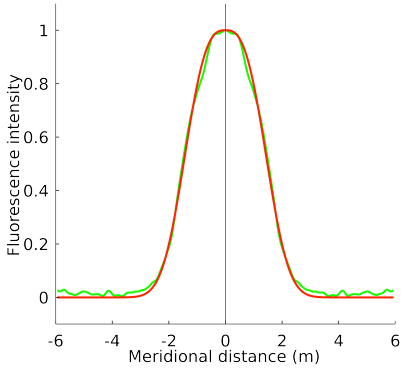

Sec6

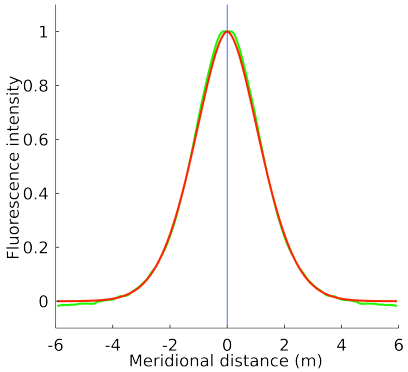

Bgs4

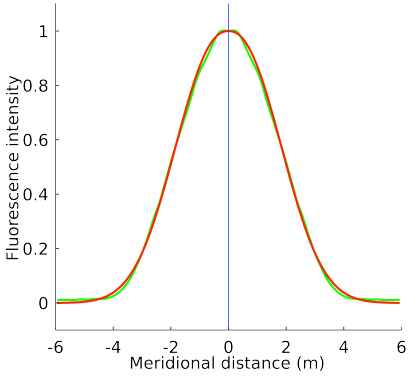

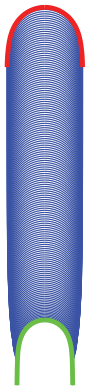

CRIB

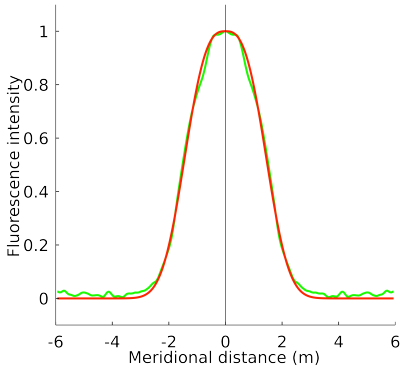

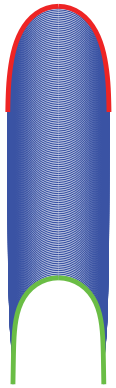

Sec6

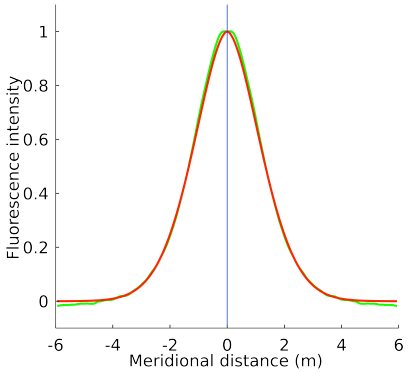

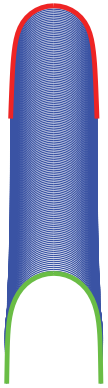

Bgs4

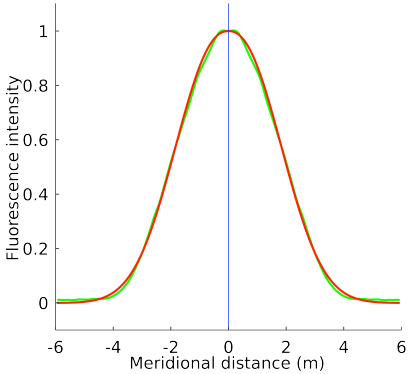

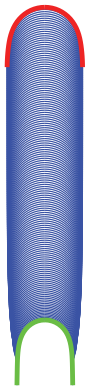

CRIB

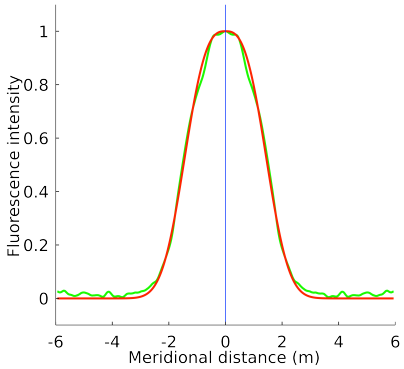

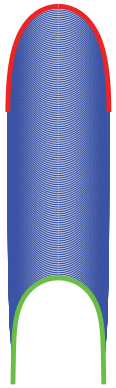

Sec6

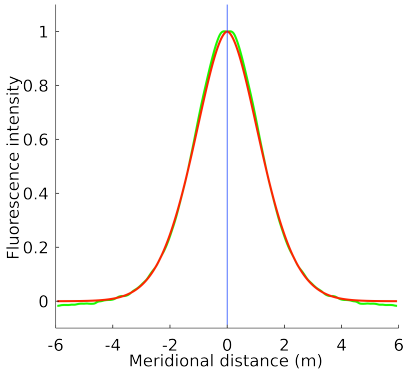

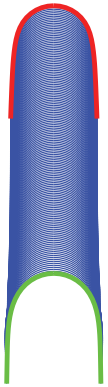

Protein	Bgs4	CRIB	Sec6
Asymptotic radius Model 1	+27%	3%	-14%
Asymptotic radius Model 2	+35%	-1%	-11%

Average radius WT:
2.01±0.03 μm (N=39)

Asymptotic meridional curvature profile

Bgs4

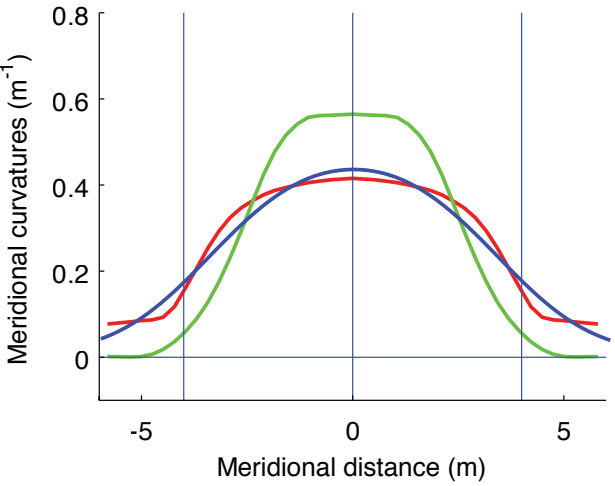

CRIB

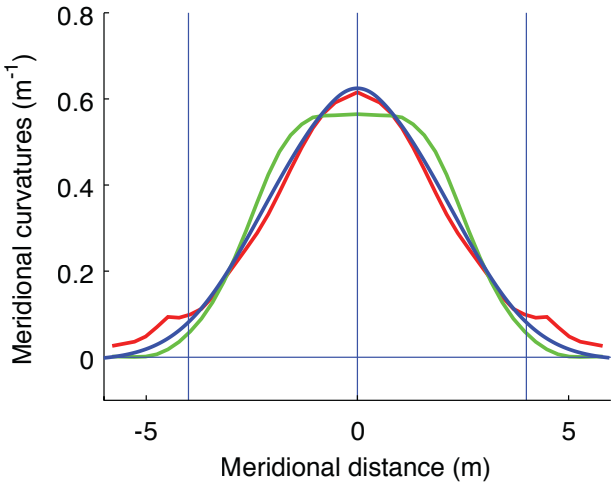

Sec6

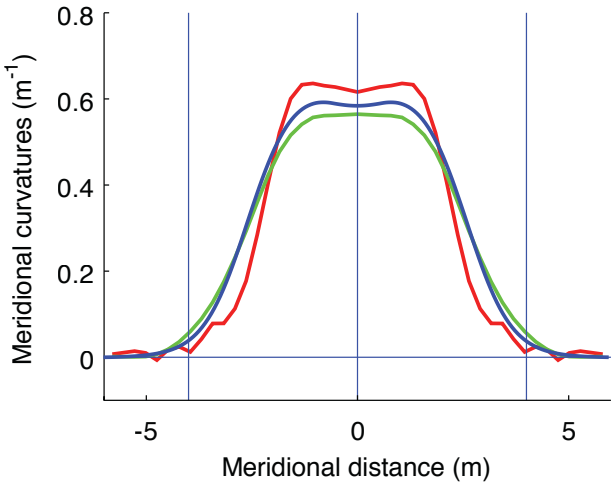

Curvature of the WT

Curvature obtained by Model 1

Curvature obtained by Model 2

Observed growth

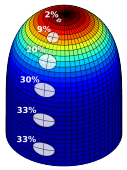

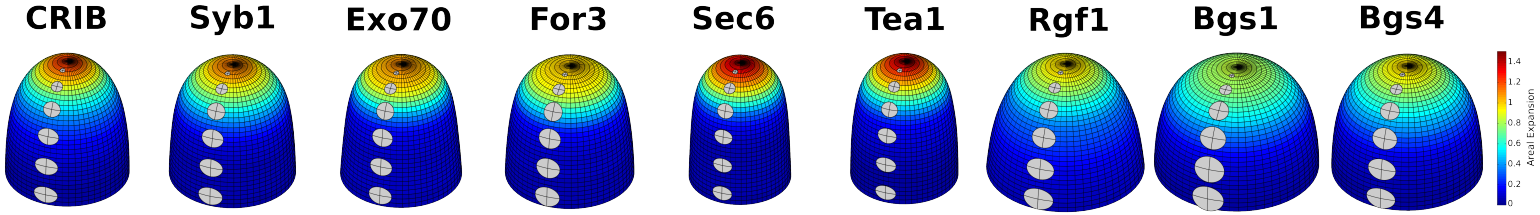

Average radius WT: 2.01±0.03 μm (N=39)

Protein	CRIB	Syb1	Exo70	For3	Sec6	Tea1	Rgf1	Bgs1	Bgs4
Asympotic radius Model 1	+11%	+14%	+9%	15%	-8%	-4%	36%	47%	36%
Asympotic radius Model 2	+6%	+10%	-5%	7%	-4%	-6%	27%	45%	45%

Growth is better predicted by proteins related to exocytosis rather than by proteins related to the synthesis of glycan.

A wider profile of Syb1, a wider cell

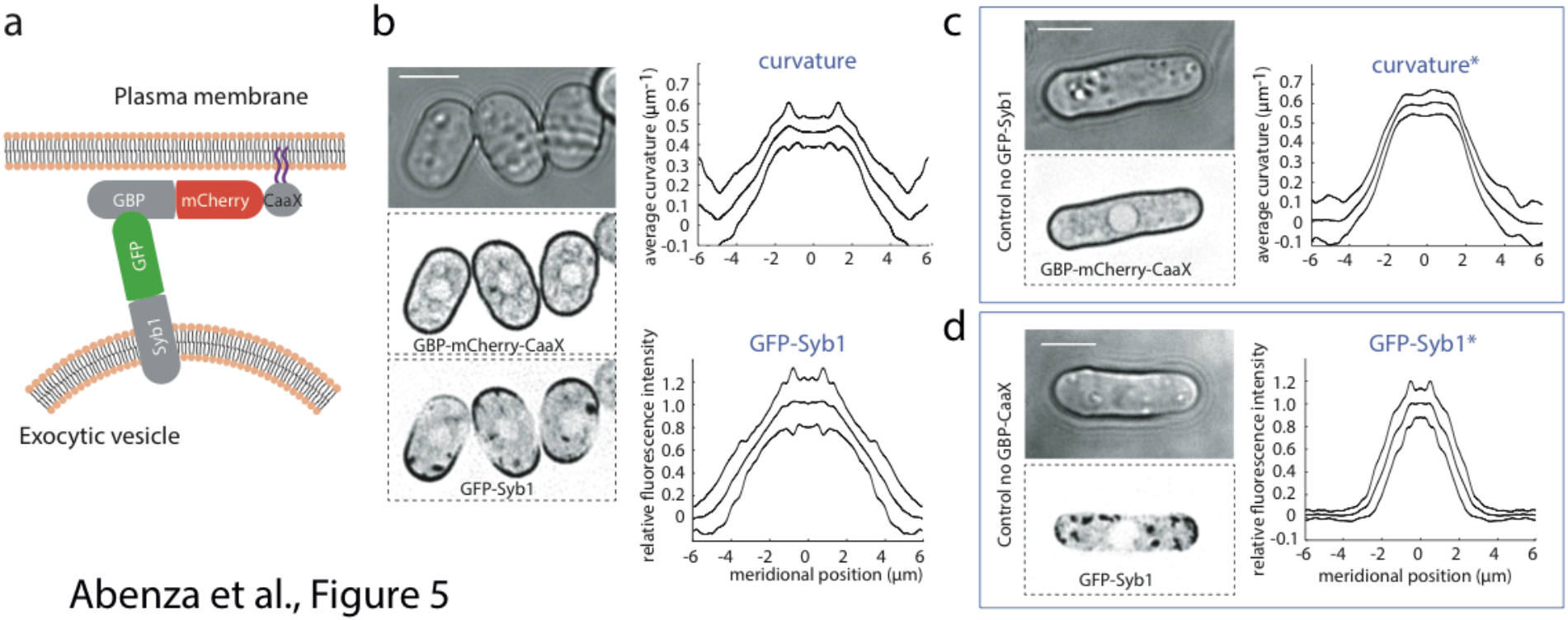

Abenza et al., Figure 5

Division scar

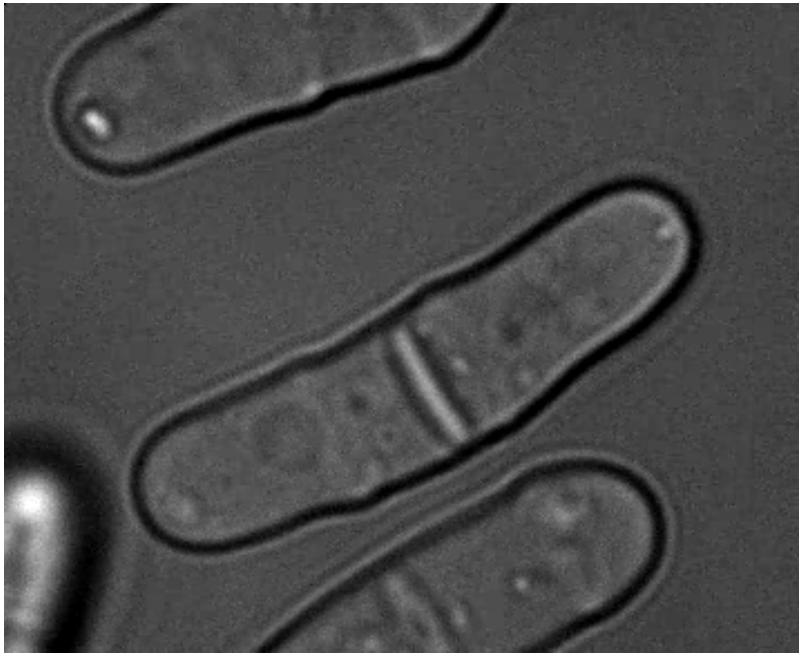

The septum (division plane) is not stretched before the division.

Division scar

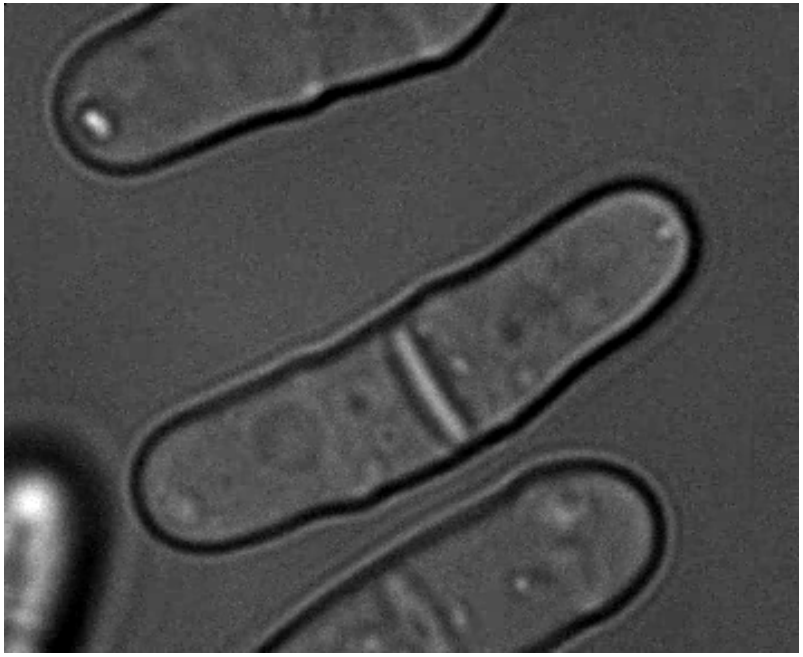

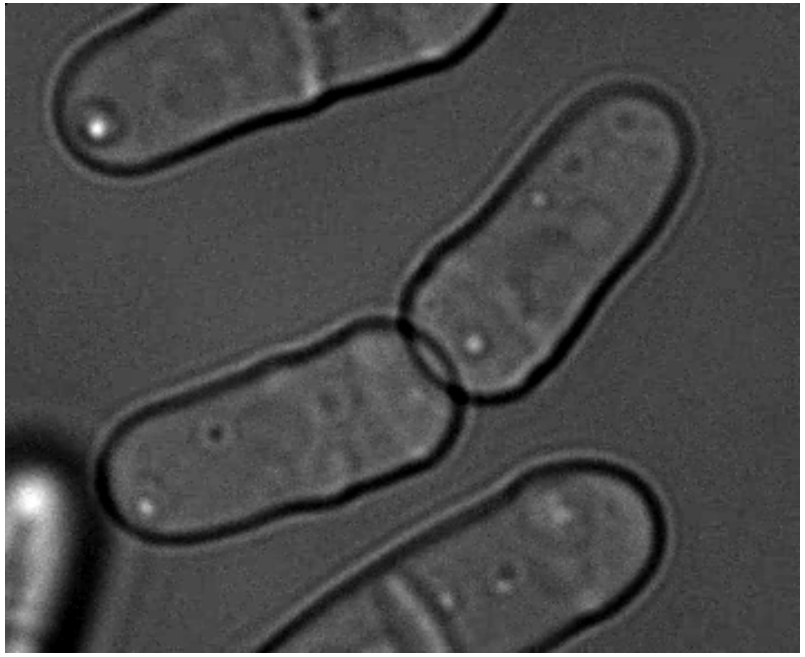

The septum (division plane) is not stretched before the division.

Model of the scar

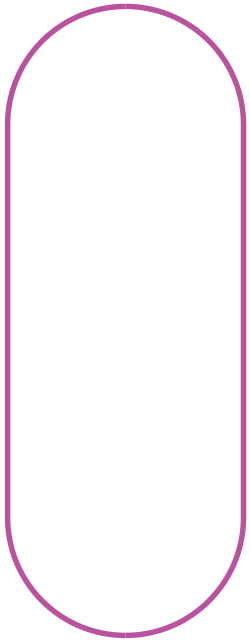

Model of the scar

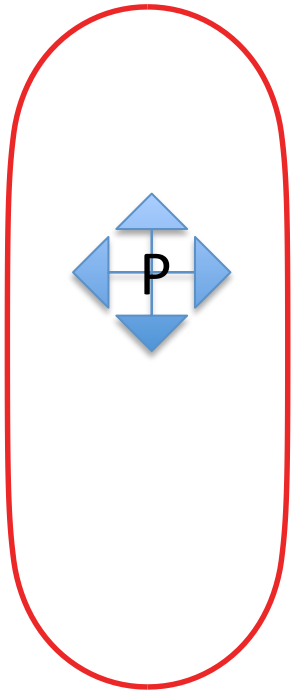

Model of the scar

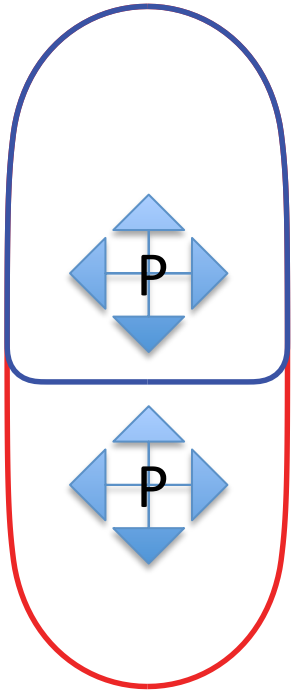

Model of the scar

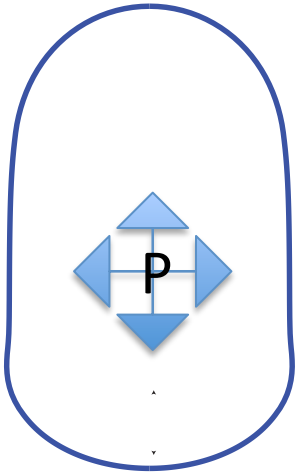

Different isotropic prestrain in the septum before the division.

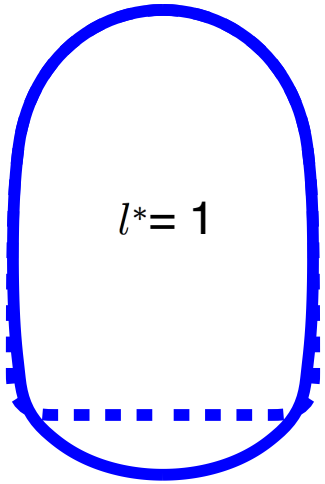

$$w(\lambda_{11}\lambda^*, \lambda_{22}\lambda^*, \gamma_2, \kappa_{11}, \kappa_{22})$$

$$\lambda^* = \frac{1}{l^*}$$

Different isotropic prestrain in the septum before the division.

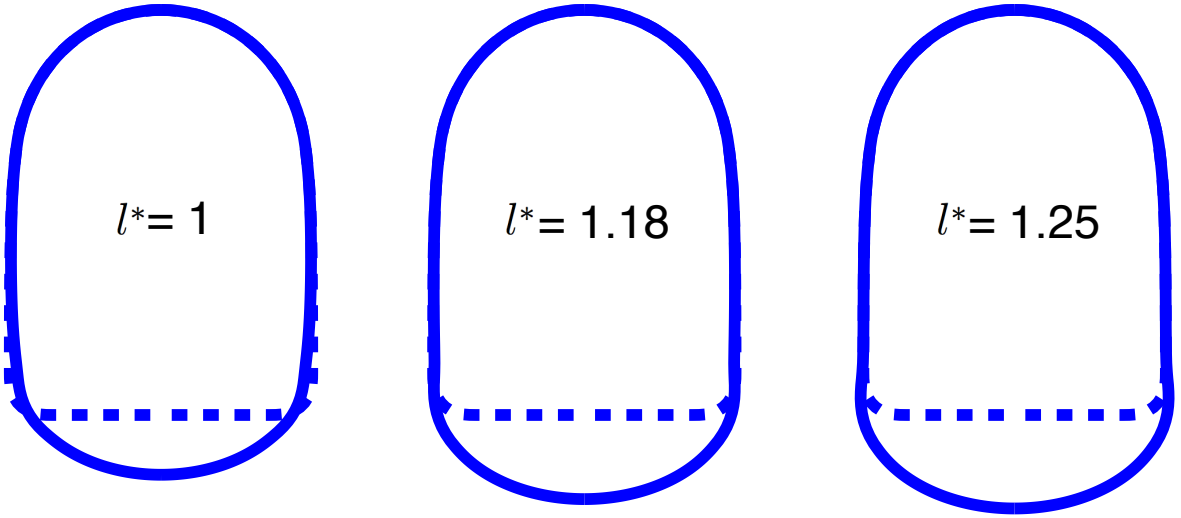

$$w(\lambda_{11}\lambda^*, \lambda_{22}\lambda^*, \gamma_2, \kappa_{11}, \kappa_{22})$$

$$\lambda^* = \frac{1}{l^*}$$

Model of the scar

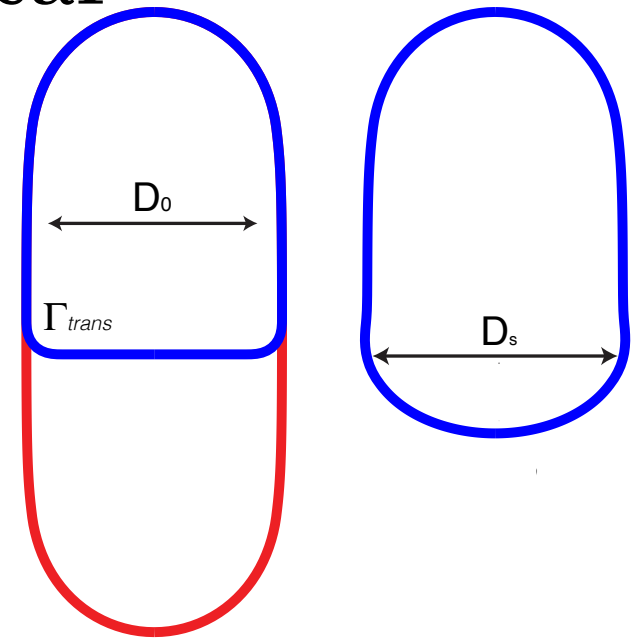

$\frac{D_s}{D_0} = 1.04 \pm 0.005$ (N= 39)

Model of the scar

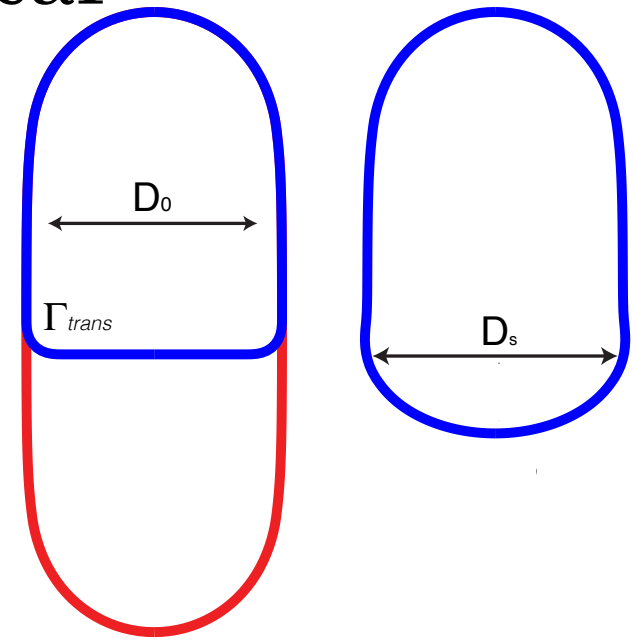

$\frac{D_s}{D_0} = 1.04 \pm 0.005$ (N= 39)

Model of the scar

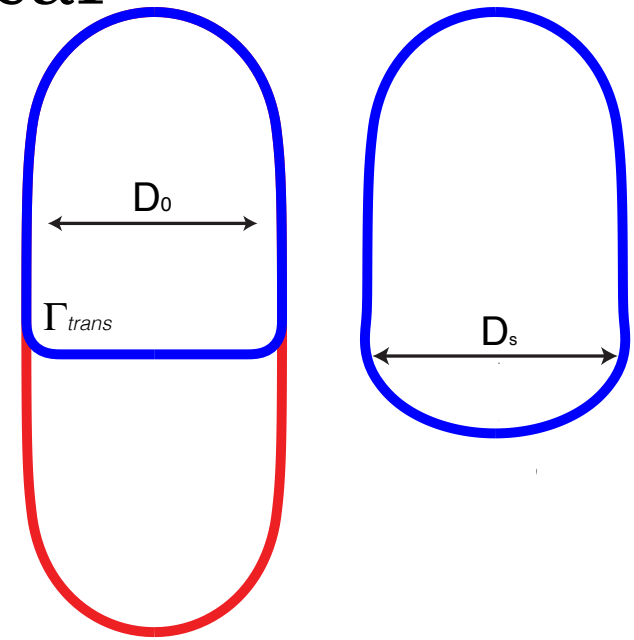

$\frac{D_s}{D_0} = 1.04 \pm 0.005$ (N= 39)

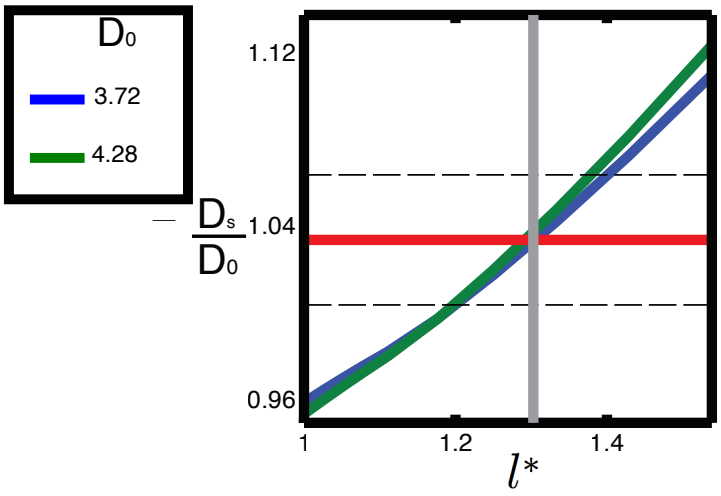

Model of the scar

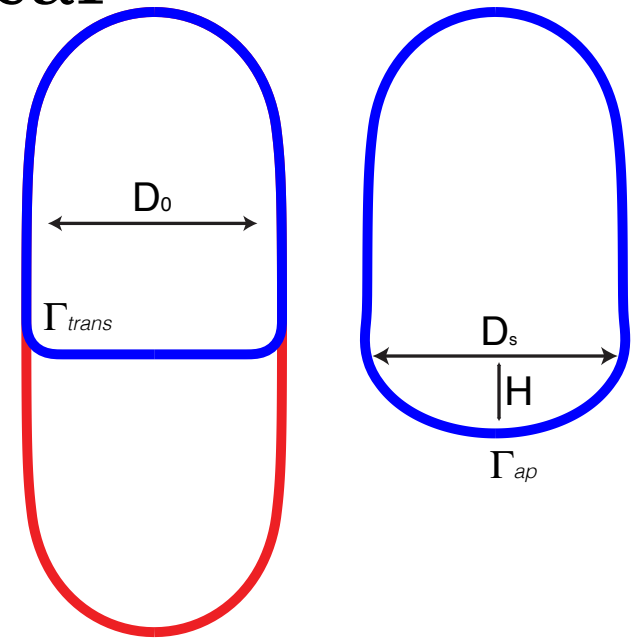

$\frac{D_s}{D_0}$ = 1.04±0.005 (N= 39)

Γ_s = 0.36±0.006 µm^{-1} (N= 39)

$\frac{H}{D_s}$ = 0.38±0.006 (N= 39)

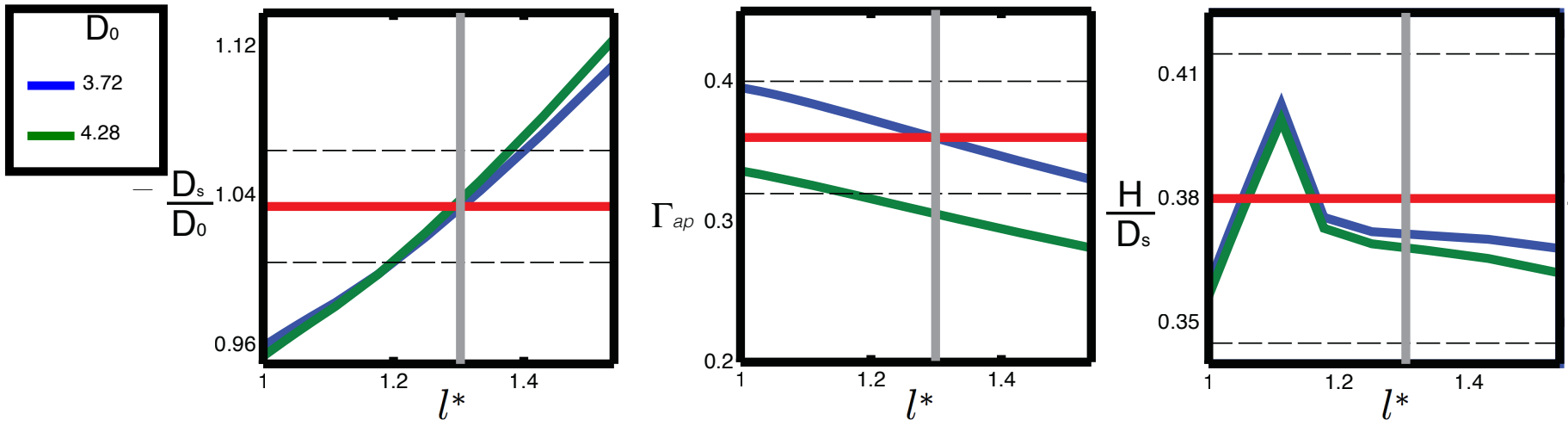

Plasmolysis

P

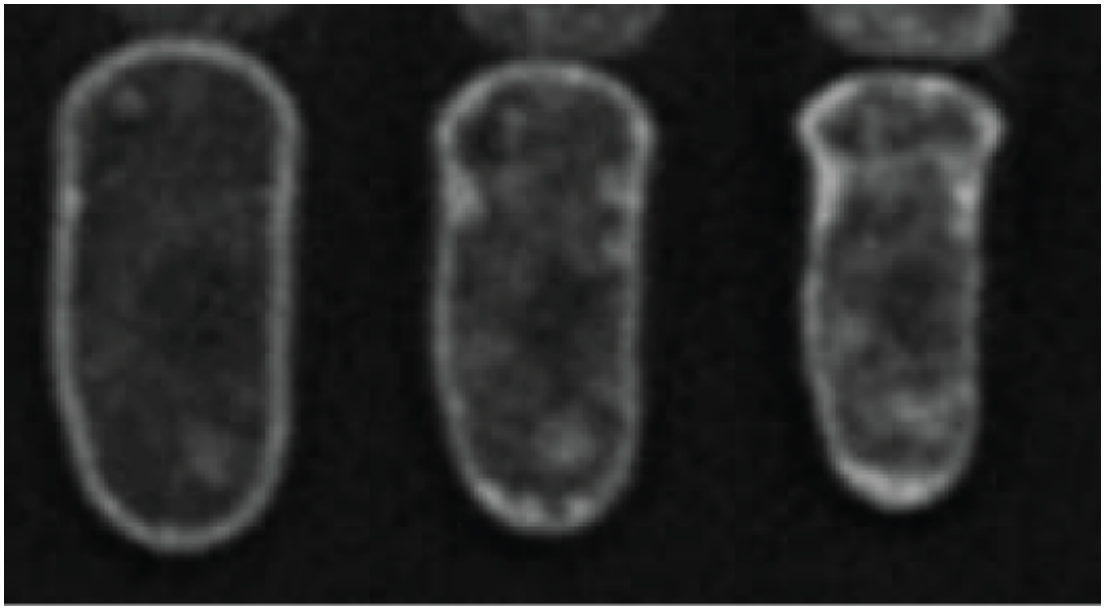

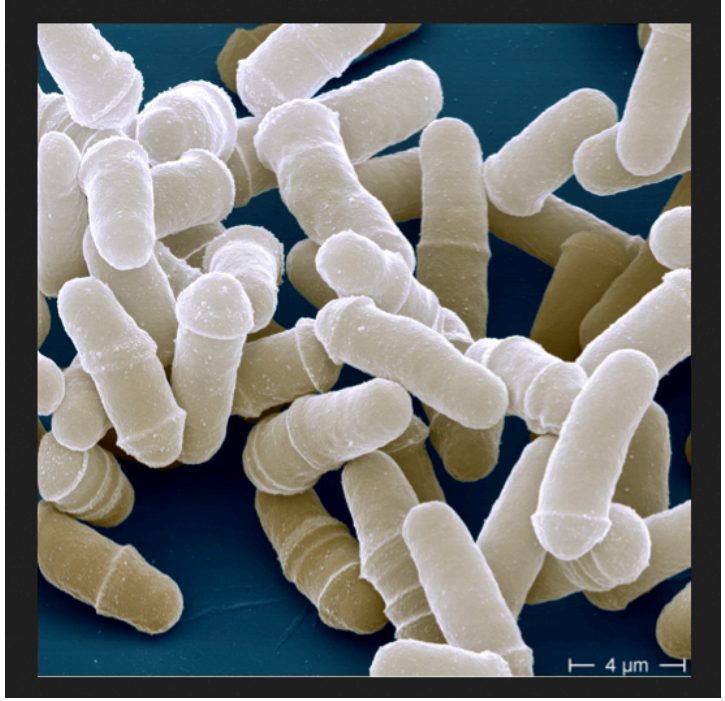

Credit Wikipedia

Conclusion :

Two models of the growth of the fission yeast combining protein localization and mechanic of the cell wall which suggest that growth is limitated rather by exocytosis than by synthesis of glycan
Ths shape of the septum after division can be explained by a rest length of the cell wall longer than one.

(Nature Communication 2015)